

Intracellular asymmetry is controlled by *JanA-1*, a polo-like kinase involved in chiral patterning within the unicellular protist, *Tetrahymena thermophila*.

Eric S. Cole^a*, Wolfgang Maier^b; Huy Vo Huynh^a; Benjamin Reister^a; Deborah Oluwabukola Sowunmi^c, Uzoamaka Chukka^c, Chinkyu Lee^c; and Jacek Gaertig^c*

^aBiology Department, St. Olaf College, Northfield, MN 55057 Electronic address:
colee@stolaf.edu and carljchmelik@gmail.com, orcid ID: 0000-0001-7353-8950

^bBioinformatics Group, Department of Computer Science, University of Freiburg, Freiburg, Germany. Electronic address: maierw@informatik.uni-freiburg.de

^c Department of Cellular Biology, University of Georgia, Athens, GA. Electronic address:
jgaertig@uga.edu

* These two authors contributed equally to the guidance of this study.

[†] To whom correspondence should be directed.

Abstract

Genetic studies on *Tetrahymena thermophila* provide a glimpse into the unexpectedly rich world of intracellular patterning that unfolds within the ciliate cell cortex. Ciliate studies draw attention away from fields of nuclei as the principal players within the metazoan pattern paradigm, focusing instead on fields of ciliated basal bodies that serve as sources of positional information and drive cortical remodeling and organelle assembly. In this study, we identify the JanA/CDC5 gene from *Tetrahymena*, and characterize its role in defining global, circumferential pattern. *JanA* is a polo-like kinase, homologous to the Human PLK3, and yeast CDC5. Loss of function results in global, mirror-duplication of ventral organelles on the dorsal surface. Gain of function (over-expression) can reduce or even eliminate cortical organelles within the ventral ‘hemi-cell’. GFP-tagging reveals that the JanA gene product decorates basal bodies strictly within the dorsal hemi-cell. These results led us to propose a model in which the default state of cortical patterning is a mirror-image assemblage of cortical organelles including oral apparatus, contractile vacuole pores and cytoproct. Dorsally-localized JanA gene product suppresses organelle assembly in the dorsal hemi-cellular cortex, resulting in a simple, ventral assemblage of these organelles, a ‘half-pattern’ as it were. PLK inhibitors produce a janus phenocopy, but reveal other unanticipated roles for PLK activities involving more local patterning events that control organelle dimensions and local organelle patterning.

Introduction

The ciliate cell-cortex during pre-division morphogenesis

Ciliated protozoa display remarkable feats of intracellular patterning through the assembly of complex organelles at precise geometric locations around the cell cortex (Cole & Gaertig, 2022; Cole, et al., 2023). In the decades between 1970 and 2000, a gallery of pattern mutants was established for the ciliate, *Tetrahymena thermophila* (reviewed by Frankel, 2008; Cole and Gaertig, 2022). Analysis of their phenotypes revealed the activity of pattern mechanisms at work driving anterior-posterior, dorsal-ventral and even left-right (chiral) asymmetry. Next-generation-sequencing has allowed us to begin identifying the gene products associated with cortical patterning in this ciliate. The first genes identified were those involved in anterior-posterior positioning of the fission zone (FZ) and the developing oral primordium (OP) (Fig. 1). Pattern genes discovered so far include members of evolutionarily conserved pathways involving

Cyclin/CDK regulation, and Hippo (Mob/Mst/ Lats) signaling (Tavares, et al., 2012; Jiang, et al., 2017, 2019, 2020).

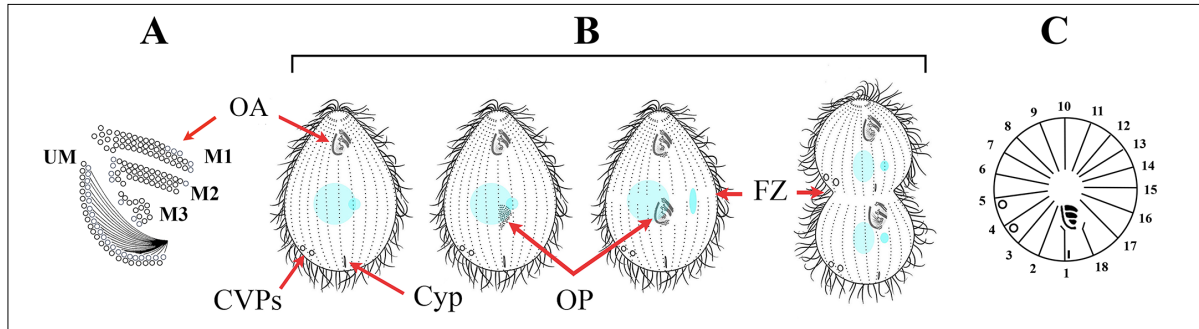


Figure 1. Schematic diagram showing cortical organelles of *Tetrahymena*. A) The oral apparatus (OA) with primary membranelles: M1, M2, M3 and the ‘undulating membrane’ or UM. B) A ventral view of a cell undergoing pre-division morphogenesis showing contractile vacuole pores (CVPs), the cytoproct (Cyp), the developing oral primordium (OP), and the fission zone (FZ). ‘Dots’ represent ciliated basal bodies assembled into ‘kineties’ or ciliary rows. C) A polar-projection of a non-dividing cell with ciliary rows depicted as lines numbered 1-18. The periphery of the circle represents the posterior end of the cell with the Cyp at kinety 1, CVPs at kineties 4 and 5, and the first post-oral ciliary row (the ‘stomatogenic kinety’) assigned the number 1. The center of the circle represents the anterior end of the cell.

Pattern formation, as studied by most modern developmental biologists, explores mechanisms that drive differential gene expression within a multicellular, multinucleate developmental landscape. *Tetrahymena* control patterning not through regulating patterns of gene expression across a multi-nucleate landscape, but through a cortical network of phosphorylation foci that broadcast pattern information from hundreds of basal bodies within a unicellular landscape. This should rightfully be viewed as a new paradigm of pattern formation.

‘Janus’ mutations represent one of the keystone phenotypes characterized within the Frankel lab (Jerka-Dziadosz & Frankel, 1979, Frankel & Jenkins, 1979). These mutants exhibit a global, mirror-duplication of the ventral pattern of cortical organelles on the dorsal cell surface. This mirror-pattern duplication is reminiscent of the *bicoid* mutant in *Drosophila*, in which embryos develop a global, mirror-duplication of the posterior half of the embryo within the anterior part of the embryo, or *gooseberry*, in which each segment exhibits a more local mirror-duplication of the posterior compartment within the anterior half-segment (Nüsslein-Volhard and Wieschaus, 1980; Frohnhofer & Nüsslein-Volhard, 1987). Janus mutations in *Tetrahymena* (for which three distinct loci have been identified) orchestrate a global, mirrored pattern-duplication of ventral organelles (oral apparatus, contractile vacuole and cytoproct) on the dorsal surface.

A second-site, janA enhancer mutation (eja)

The original janus mutant (*janA*), was isolated in the very first attempt to isolate temperature-sensitive cell-division mutants from *Tetrahymena* (Bruns & Sanford, 1978). From a cell culture mutagenized by exposure to nitrosoguanidine and made homozygous through a form of self-fertilization called ‘short circuit genomic exclusion’ (Bruns, et al., 1976), a clone with enlarged, and somewhat ‘flattened’ features was isolated (CU127). This mutant clone was initially identified due to its high mortality following prolonged growth at elevated temperature (39.5 C). The cell’s cortical features were subsequently analyzed using traditional silver-impregnation staining (Frankel & Heckmann, 1968; Nelsen & DeBault, 1978). CU127 cells exhibited an elevated number of ciliary rows (21-25 in the mutant vs 17-21 seen in a wildtype clone) while 50% of the mutant cells exhibited two sets of CVPs, and 30% exhibited a secondary oral apparatus located 180 degrees around the circumference from the first, ‘normal’ set. This mutant was later named *janA-1* (Jerka-Dziadosz & Frankel, 1979).

Genetic analysis revealed that *janA-1* was recessive, mapped to the right arm of chromosome 3, and appeared to require a second-site enhancer mutation (*eja*: enhancer of *janA*) for elevated penetrance (Frankel and Jenkins, 1979). Subsequent rounds of mutant screening recovered a 2nd allele that failed to complement the first (*janA-2*).

The janus cortical phenotype and its developmental emergence

Taking advantage of *Tetrahymena*’s unique genetics (a somatic, transcriptionally active macronucleus and a transcriptionally silent germline micronucleus), Frankel and Nelsen (1985) were able to observe the progressive emergence of the janus, loss-of-function phenotype against an initially wildtype background. During cell division, the anterior division product of a ciliate (the ‘proter’) inherits the parental OA and assembles a new set of CVPs, while the posterior division product (the ‘opisthe’) inherits the parental CVPs while assembling a new OA (Fig. 2, upper panel).

At each cell division, one observes both the ‘inherited’ organelles of the parent cell, and newly assembled organelles. Following genetic replacement of the wildtype macronucleus with one homozygous for the *janA* mutation, cells are initially wildtype, but as cell-divisions proceed, any residual wildtype JanA gene product is either diluted or broken down over time. Consequently, successive cell divisions reveal cortical patterning under conditions with progressively less of the wildtype product.

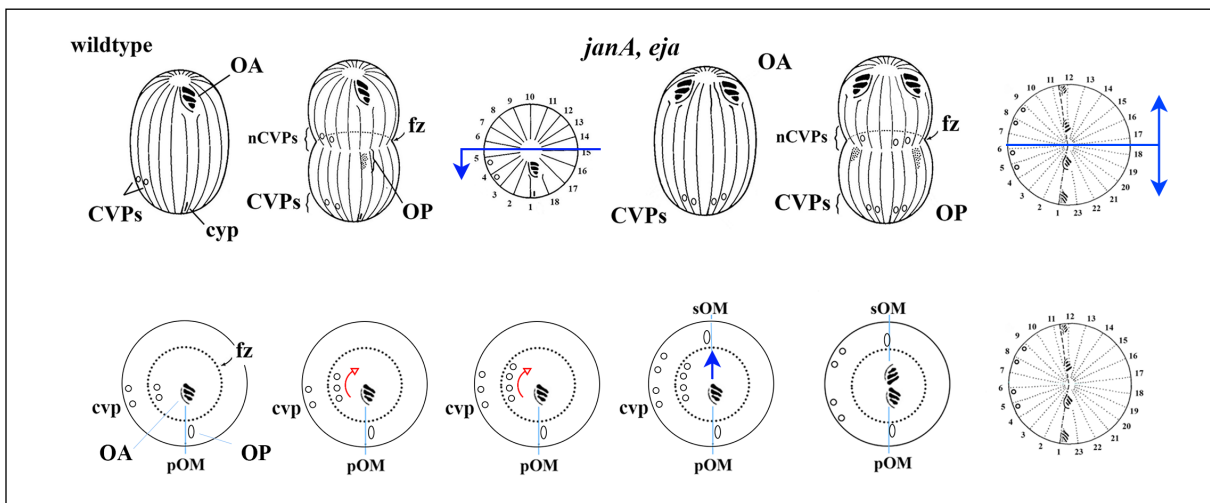


Figure 2. Cortical landmarks during pre-division morphogenesis in a wildtype and a *janA, ejA* double-mutant. The top panel depicts wildtype and mutant *Tetrahymena* cell in a variety of highly stylized ways: a ventral diagram of a non-dividing cell, a ventral diagram of a dividing cell as new organelles are assembled, and a ‘polar projection’ view of a non-dividing cell. OA = the oral apparatus. OP = the developing (‘new’) oral primordium. FZ = the fission zone. CVPs = contractile vacuole pores. nCVPs = ‘new’ contractile vacuole pores. Linear stripes represent longitudinal rows of ciliated basal bodies. The ciliary rows are numbered in the polar view with the oral meridian (the ciliary row that gives rise to the next oral apparatus), numbered as one, and numbers increasing in a clockwise fashion looking down from the anterior pole. The blue arrow demarcates the wildtype dorsal hemi-cell (above the line) from the ventral hemi-cell within which the more complex cortical organelles assemble (below the line). In the most extreme janus phenotype, the ventral pattern is duplicated with mirror-symmetry in the dorsal hemi-cell (indicated by blue arrows).

The bottom panel depicts polar projections of a dividing wild-type cell from which the *JanA* gene product has been effectively removed (within an *eja*- genetic background) and the cortical phenotype observed through subsequent cell generations. The dotted circle represents the fission zone with the oral primordium assembling just posterior to it alongside the primary oral meridian (pOM), and new CVPs assembling just anterior to the fission zone, and to the cell’s right of the pOM, approximately 90 degrees. The janus phenotype is first evident as a broadening of the CVP domain from two to three and finally four CVPs (curved red arrows). This broadening manifests in newly formed CVPs anterior to the FZ. Only after full CVP broadening does the secondary OP assemble along the secondary oral meridian (sOM, blue arrow), manifesting the most extreme form of the phenotype, a mirror-image duplication of the wildtype, ventral pattern of cortical organelles.

The result is first a broadening of the CVP domain from two to three or four organelles followed by a split in the CVP domain, effectively creating two CVP domains separated by one or more ciliary rows. Finally, following the broadening and ‘duplication’ of the CVP domain, a secondary OP assembles approximately 180 degrees from the primary OA (Fig. 2 Lower panel). The fully expressed mirror-duplication only appears in 30-50% of the population, and only under the influence of the 2nd site enhancer, *eja*.

The *janA* mutant phenotype is clearly complex, hinting at a corresponding wildtype gene with an equally complex role during vegetative development. This study identifies the *JanA* gene, documents both deletion and over-expression phenotypes, characterizes localization of the

gene product (via imaging of a JanA:GFP fusion product during vegetative development), and documents a pharmacological phenocopy of the pattern mutant. Results are discussed with reference to the phenomenon of chiral, circumferential patterning in the *Tetrahymena* cell cortex ('C-Patterning')

Results

Identifying the *JanA1* gene

The *janA-1* mutation was mapped to the right arm of micronuclear chromosome 3 using complementation tests in crosses to nullisomic strains lacking specific micronuclear chromosomes (Bruns and Sanford, 1978; Bruns, et al., 1983; Cassidy-Hanley, et al., 1994; Frankel and Jenkins, 1979). We used 'allelic composition contrast analysis' (ACCA) (Jiang et al., 2017), to map the causal mutation for *janA* (see Jiang ???, Cole, et al., 2023). Briefly, we sequenced pooled genomes of F2 progeny that were homozygous for either the *janA-1* or wild-type alleles. For each sequence variant, scores were computed that reflect the extent of linkage to the mutant phenotype and these were plotted against genomic coordinates of the five micronuclear chromosomes. A peak of increased linkage was apparent on chromosome 3 around a ~25.5 mb position (Fig. 3).

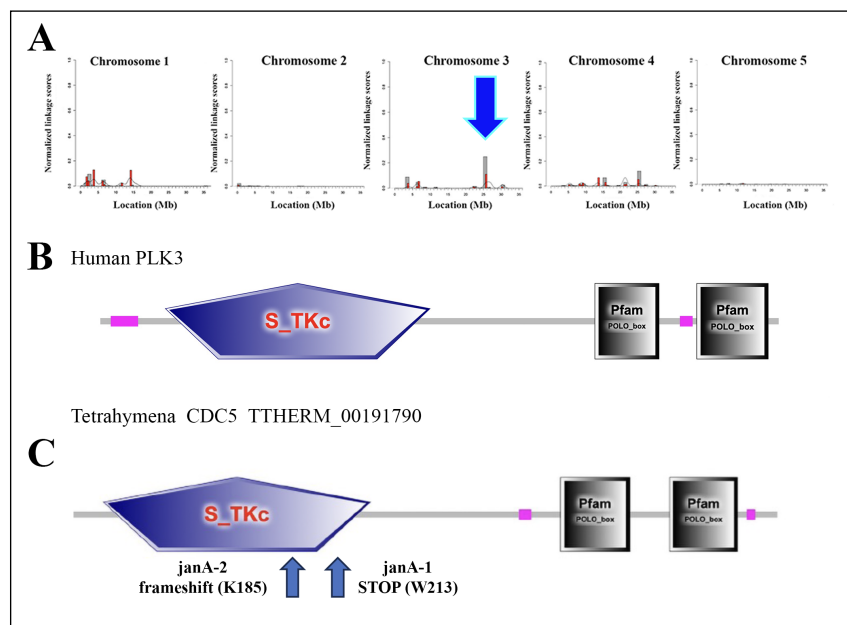


Figure 3. The *janA1* alleles map to TTHERM_00191790, a gene that encodes a conserved polo-like kinase (PLK) similar to the yeast gene, CDC5. domain protein. (A) Mapping the *janA1* mutation using the ACCA workflow of comparative whole genome sequencing (see methods). The scores reflect the degree of linkage of sequence variants to *bcd1-1* among the meiotic F2 segregants. Note increased linkage signal on chr 3 around the position 25.5 mb. (B,C) A comparison of the domain organization of TTHERM_00191790/JanA-1 and its likely human ortholog PLK3. Arrows indicate approximate sites of two nucleotide alterations associated with the two mutant isolates.

Within this genomic region, there was a premature stop codon in the gene locus TTHERM_00191790 in the *janA-1* mutant strains. BLASTp searches revealed that the TTHERM_00191790 protein exhibits strong amino acid sequence homology to Human PLK3, and yeast CDC5. A second mutation conferring essentially the same ‘janus’ phenotype, maps to the same chromosome arm, and fails to complement the *janA-1* mutation. This was therefore designated the *janA-2* allele. PCR and sequence analysis demonstrated that the TTHERM_00191790 locus of the *janA-2* allele, contains a base pair deletion resulting in a frame shift (Fig. 3, See Suppl. Fig. 1). The *janA-1* and *janA-2* mutations result in truncation of large portions of the protein including both of the polo-box sequences, suggesting that *janA-1* and *janA-2* are null alleles.

To further validate TTHERM_00191790 as the *JanA* locus, we targeted a portion of the coding region of TTHERM_00191790 (from ### to ###) for deletion in a wildtype strain using a scan RNA based ‘codeletion’ approach (Hayashi & Mochizuki, 2015). A codel transformant clone carrying a deletion within TTHERM_00191790 was evaluated by immunofluorescence using anti-centrin and anti-fenestrin antibodies to image the cortical organelle patterns. Curiously, the co-deletion clones showed only a mild form of the mutant phenotype, a broadening of the CVP domain, with no examples of global mirror-pattern duplication. The deletion was then introduced to the cell-line IA264 (mating type II). This strain is homozygous for *eja*, the ‘enhancer of *janA*’, a 2nd-site mutation that has been shown to intensify the janus phenotype in *janA-1* mutant cell lines. These transformants exhibited the most extreme form of the janus phenotype including 30-40 % of the cells displaying the complete mirror image pattern duplication.

With these proofs: base-pair alterations in the TTHERM_00191790 gene within both *janA-1* and *janA-2*, and the full mutant phenotype exhibited by the targeted deletion of this gene in an *eja*-dependent fashion, we were confident that we had identified the relevant *JanA* gene.

The janus cortical phenotype

We first examined a co-deletion of the TTHERM_00191790 gene within a wildtype genetic background (strain CU428). Using an antibody to centrin, we saw no evidence of a duplicated oral apparatus or oral primordia (Fig. 4A). Upon labeling of the CU428 deletion strain with an antibody generated against the cortical protein fenestrin, (an antibody that decorates CVPs among other cortical features), we saw evidence of a weak *janA* phenotype, a broadened CVP

domain, and rarely a duplicate pair of CVP domains (Figs. 4 B, C). We then disrupted the TTHERM_00191790 gene within the IA264 cell line, homozygous for the ‘enhancer of janA’ (*eja*). Among these cells, we saw approximately 30-40% of the cells exhibiting the full, mirror-duplication phenotype with two OAs and OPs located 180 degrees opposite one another (Fig. 4F). Being able to recreate the *janus* phenotype by co-deletion of the TTHERM_00191790 locus provides further compelling evidence that we have in fact identified the *JanA/CDC5* gene in *Tetrahymena*.

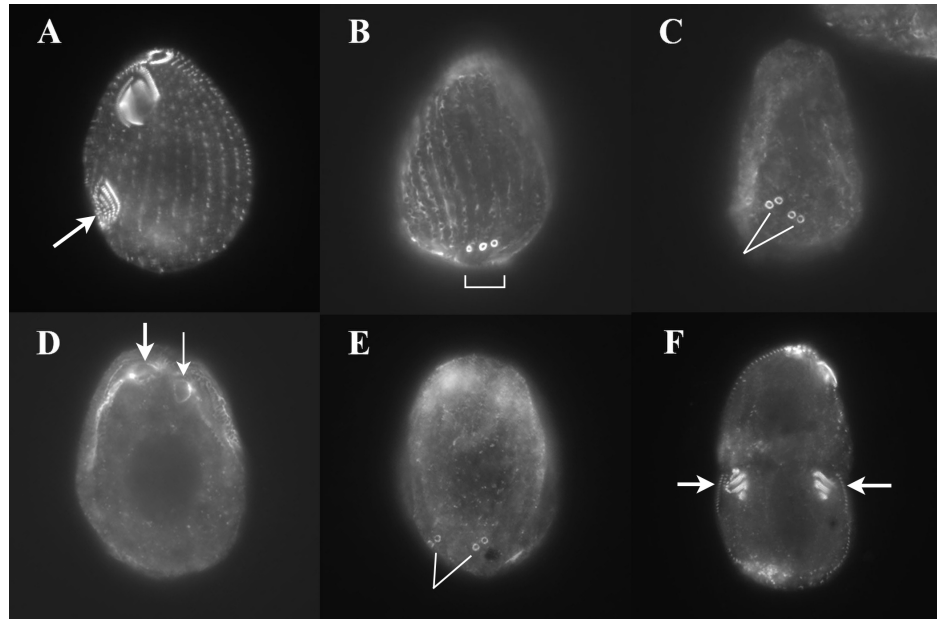


Figure 4. Cells in which we targeted TTHERM_00191790 for gene-disruption and labeled with cortical antibodies. A-C). A CU428 (Wildtype) cell line labeled with A) anti-centrin antibody targeting basal bodies, we only saw cells with a single OA and OP (arrow), and B,C) an antibody to the protein fenestrin (that decorates CVPs) revealing the ‘mild’ *janA* phenotype with CVP broadening (B), bracket, and occasionally a split, dual CVP field (C), lines. When the locus was disrupted in IA264 (a cell line homozygous for *eja*) we recovered the more extreme-mirror phenotype (D-F). D, E) The same *janA* co-deletion cell labeled with antibody to fenestrin revealing twin OAs on one side (D, arrows) and twin CVP sets on the other side (E, lines). Note: fenestrin does a poor job high-lighting the OA so cells were also labeled with anti centrin revealing a proper twinned set of OAs and OPs (F arrows) representing the extreme Janus phenotype.

The JanA-1 expression profile.

Curiously, the *Tetrahymena* JanA/CDC5 gene shows peak expression, not during vegetative growth and division (when the patterning occurs that led to the initial discovery of the mutant), but during conjugal development. In particular, we see peak expression during meiosis and recombination (2-4 hrs into mating), and during macronuclear anlagen formation (between 6-12 hours of mating). See Figure 5. The published expression data drew our attention to possible JanA functions during conjugation (a study being prepared separately). The present study

focuses on the expression, localization, and phenotypic defects associated with the pre-division morphogenesis and cortical patterning exhibited during vegetative growth and development.

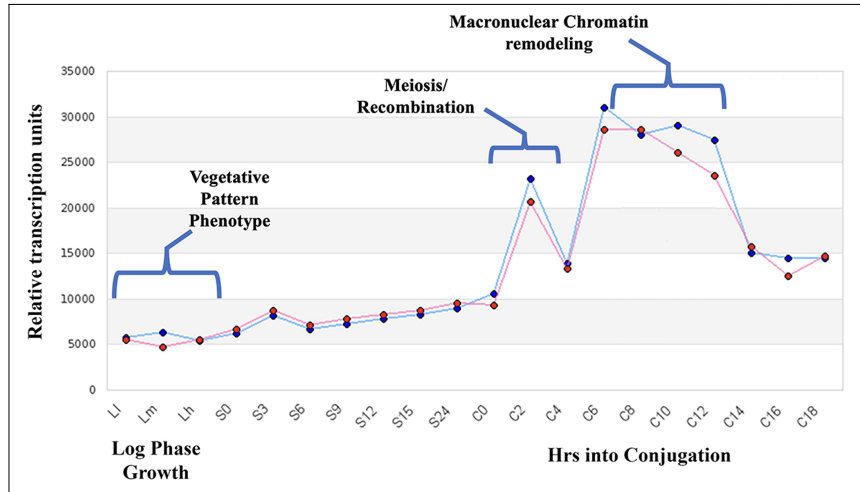


Figure 5. Expression profile of mRNA for JanA/CDC5 (TTHERM_00191790) obtained from the Tetrahymena Functional Genomics database (http://tfgd.ibh.ac.cn/search/detail/gene/TTHERM_00191790). The levels of mRNA at the following conditions are shown: L-l, L-m and L-h: vegetatively growing cells collected at $\sim 1 \times 10^5$ cells/ml, $\sim 3.5 \times 10^5$ cells/ml and $\sim 1 \times 10^6$ cells/ml. S-0, S-3, S-6, S-9, S-12, S-15 and S-24: cells starved for 0, 3, 6, 9, 12, 15 and 24 hours. C-0, C-2, C-4, C-6, C-8, C-10, C-12, C-14, C-16 and C-18: conjugating cells collected at 0, 2, 4, 6, 8, 10, 12, 14, 16 and 18 hours after initiation of conjugation by mixing different mating types.

Localization of a JanA-GFP fusion product driven from the endogenous JanA promoter.

The *JanA/CDC5* gene was fused to a GFP coding sequence, cloned downstream from the cell's endogenous *JanA/CDC5* promoter, and expressed in live *Tetrahymena* cells during vegetative cell growth (Fig. 6).

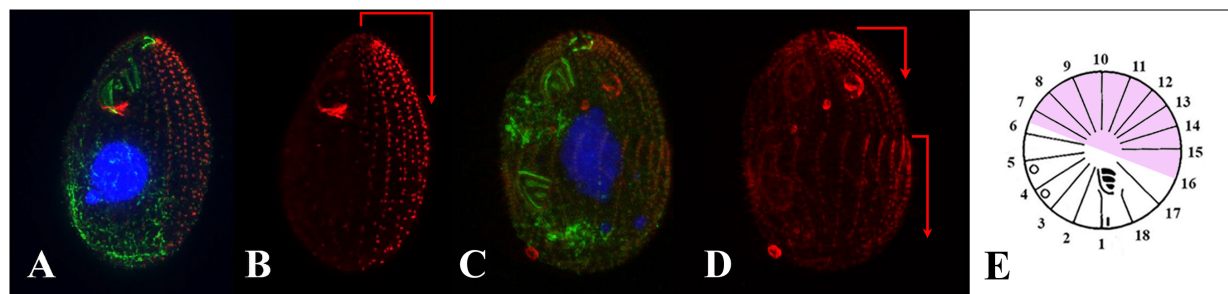


Figure 6. *Tetrahymena* cells expressing a JanA/CDC5:GFP fusion protein from the endogenous promoter during vegetative cell division and development. Cells were fixed, and GFP-localization was enhanced using an antibody to GFP with a TRITC-tagged secondary antibody (RED). Cells were counter-stained using antibody to centrin with a FITC (green) secondary antibody. A) A double-labeled cell during interphase showing the OA and basal bodies (green) and the JanA/CDC5:GFP fusion protein (red). Note: anti-centrin also decorates a rich cytoplasmic network associated with the contractile vacuoles: green matrix in lower left of cell. Nuclei were labeled with DAPI. B) The same cell showing just JanA/CDC5:GFP localized to basal bodies strictly in the 'dorsal hemi-cell' (arrow). C, D) Similar labeling of a cell undergoing pre-division oral morphogenesis. E) Polar projection showing the dorsal hemi-cell (pink) within which JanA:GFP protein appears localized around corresponding basal bodies.

The JanA/CDC5:GFP fusion protein seems to be closely associated with basal bodies but strictly in the dorsal hemi-cell from 10:00, (7th ciliary row), to 4:00 (16th ciliary row) moving clockwise and viewing the polar-projection with the post-oral meridian (row # 1) defining 6:00 (See Fig. 6E for reference). It is significant, that the cortical domain occupied by wildtype JanA/CDC5 protein defines the region where the mirror-duplication of ventral organelles is manifest in the loss-of-function mutants.

JanA/CDC5:GFP driven by an inducible promoter (2-4 hrs) provides a stunning fluorescent marker of the entire cortical landscape, a ‘cortical pattern reporter’.

The JanA/CDC5:GFP fusion gene was then cloned downstream from the cadmium-inducible *MTT1* promoter (Shang *et al.*, 2002), and expressed in live *Tetrahymena* cells during vegetative cell growth (Fig. 7). The MTT1 promoter is ‘leaky’ driving a modest level of expression even without cadmium present in the environment. With zero cadmium added to the growth medium, one observes the same pattern of basal body localization restricted to the dorsal hemi-cell as observed using the endogenous promoter (See Fig. 6A). When cells carrying the MTT:JanA/CDC5:GFP fusion gene are exposed to cadmium chloride (2.5 ug/mL) for 2-4 hrs, fluorescence localization spreads to all the basal bodies (both dorsal and ventral), the developing oral primordium (OP) and mature OA, and the CVPs. As such, this construct represents a potentially powerful tool for the study of cortical architecture, pattern formation and development in live *Tetrahymena*.

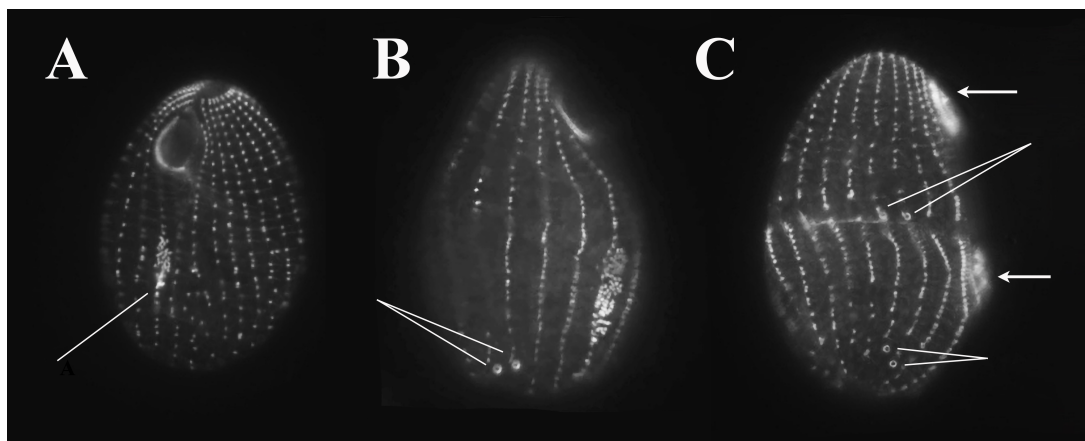


Figure 7. Wildtype (CU428) cells expressing the inducible JanA/CDC5:GFP fusion protein following 4 hours of exposure to 2.5 ug/mL cadmium chloride. A) All the basal bodies (dorsal and ventral) are now decorated including the basal body proliferation field that marks assembly of the OP (thin arrow). B) A similarly labeled cell undergoing pre-division oral morphogenesis, showing the typical pair of CVPs (thin arrows). C) A slightly later stage in pre-division morphogenesis showing the fully developed OP and OA (thick arrows) and the old and new CVPs (thin arrows), new CVPs forming just anterior of the developing cytokinetic furrow.

It should be noted that prolonged expression of the GFP-fusion gene (beyond 6 hrs) leads to a progressively more severe over-expression phenotype (see below). That said, cells exposed for 2-4 hrs, or pulse-chased with cadmium (again for under 4 hrs) appeared phenotypically normal (Fig. 7).

An over-expression phenotype from continuous JanA/CDC5:GFP fusion gene expression.

As mentioned earlier, driving the JanA/CDC5:GFP fusion protein from the endogenous promoter, or from an inducible, cadmium-driven MTT1 promoter in the absence of cadmium-induction, produces cells that exhibit basal body labeling strictly over what we are referring to as the dorsal hemi-cell (between 10:00 and 4:00 in the polar, clock representation). We have inferred that this is likely the normal distribution of the JanA gene product in wildtype cells.

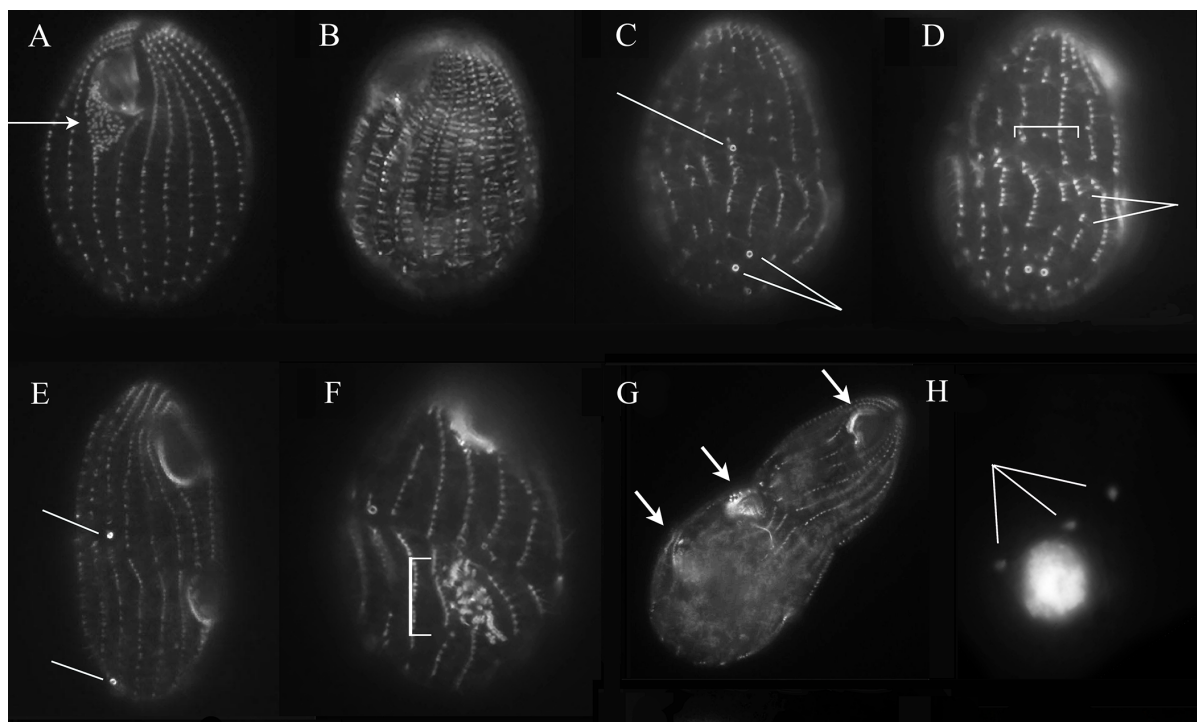


Figure 8. Wildtype (CU428) cells expressing the inducible JanA/CDC5:GFP fusion protein following 5-28 hours of exposure to 2.5 μ g/mL cadmium chloride. A) After 5 hrs, we witnessed a wave of ‘oral replacement’, a process typically triggered (in untreated cells) by starvation. B) After 6-8 hrs. of cadmium-induction, janA/CDC5:GFP began to decorate the transverse microtubules. C, D) Cells that divided after 6-8 hrs of induction began to exhibit a reduction in the breadth of the CVP domain from the typical two to one (Fig. C) to zero (Fig. D, bracket). Breaks also began to appear in the ciliary rows of basal bodies (white pointers). E) Fenestrin-labeled cells incubated overnight with cadmium exhibited a reduction in both the mature CVP domain (lower pointer) and the developing domain (upper pointer). F) Centrin-labeled cells began to exhibit disruptions in oral assembly (bracket). Membranelles appear to be forming in a variety of orthogonal relationships with no distinct UM. G, H) Overnight induction of the JanA/CDC5:GFP fusion protein produced cells arrested in cell division. G) A centrin-labeled cell showing three OAs (arrows) and H) the same cell with DAPI label revealing multiple MICS (pointers) but no MAC division.

Cells expressing fusion protein at these levels exhibit normal phenotypes with a single OA and a single pair of CVPs. Upon addition of 2.5 ug/mL CdCl₂, the induced GFP-fusion protein distribution begins to change, decorating all the basal bodies as well as the CVPs. As such, cell lines carrying the inducible construct represent an excellent new resource for those studying cortical events in *Tetrahymena*. During the four hours immediately following induced JanA/CDC5:GFP expression, cells expressing this construct show only one conspicuous abnormality. After two hours of induced over-expression, cells begin to undergo '***oral replacement***' (Fig. 8A). Oral replacement has been characterized as a starvation response (Frankel, 1969; Nelsen, 1978; Williams & Frankel, 1973).

Oral replacement is first detected when the posterior half of the Undulating Membrane (UM) and the anterior-most basal bodies of the post-oral ciliary row become disorganized, and form a replicative field of basal bodies that eventually establishes a new replacement OA. The population of cells that undergo oral replacement in response to *JanA/CDC5:GFP* over-expression is quite high, with 50% of the population undergoing this alternative development after 5hrs (Fig. 9). This suggests, that virtually the entire population may carry out oral replacement in response to exogenous *JanA/CDC5* fusion-gene over-expression.

After four hours of continuous over-expression, we began to observe a suite of abnormalities (See Fig. 8). First, JanA/CDC5:GFP localization spread from the basal bodies to the transverse microtubules (Fig. 8 B). At the same time, cells undergoing cell-division begin to exhibit a

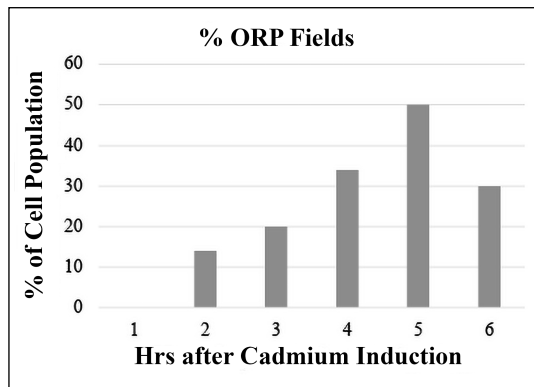


Figure 9. The percentage of a population undergoing oral replacement at a given time following initiation of CdCl₂-induced JanA/CDC5:GFP expression from the MTT1 inducible promoter. This is a representative data set collected from a single experiment.

reduction in the breadth of the new CVP domain from 2 to one, and even zero, though such examples were only observed in the anterior division product prior to cytokinesis. Daughter

cells that have completed division lacking a CVP are presumably unable to osmoregulate and die (Figs. 8 C-E). Some cells began to exhibit fragmentation of the ciliary rows (Fig. 8 D) and with prolonged *JanA/CDC5* over-expression, the OP exhibits signs of pattern derangement (Fig. 8 F). After six hours, over-expression cells exhibit difficulties with mitosis, especially MAC division and cytokinesis. Curiously, MIC division and stomatogenesis seem relatively unaffected resulting in cells with multiple OAs, multiple mics, but only one or at most two MACs (Figs. 8 G-H). These cells also appear to continue to replicate their basal bodies.

Multi-polar Tetrahymena following over-expression of the JanA/CDC5:GFP fusion protein.

Between 8 and 24 hrs of cadmium-induced over-expression, and following multiple failed rounds of cytokinesis, some cells assume a configuration in which there appears to be one anterior pole and multiple posterior poles (Fig. 10). In Figure 10, the red arrows indicate CVPs (and the presumptive posterior) while blue arrows highlight the OAs and the presumptive anterior end of the cell.

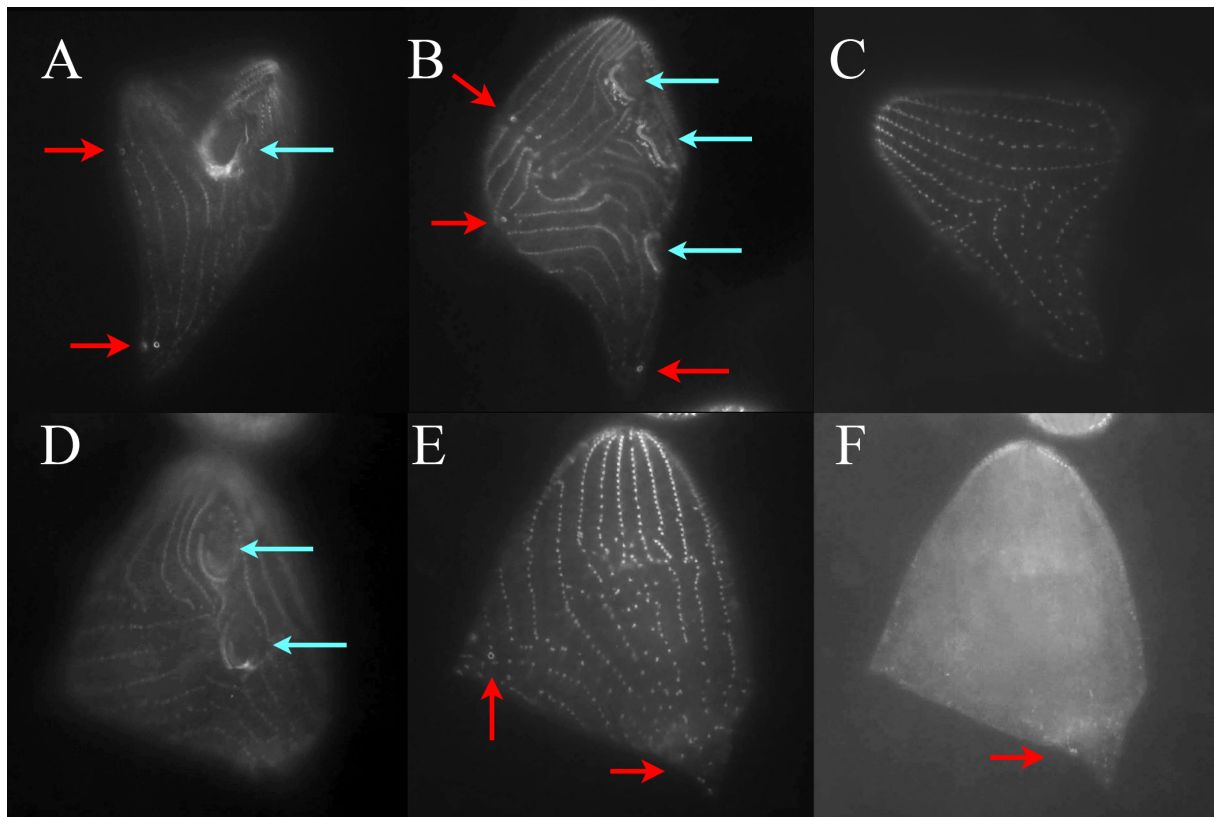


Figure 10. *Tetrahymena* cells following 8-24 hours of induced over-expression of the *JanA/CDC5:GFP* fusion protein. Red arrows indicate CVPs (and a presumptive posterior pole) while blue arrows indicate OAs (and the presumptive anterior pole). A-C) represent individual cell morphologies. D-F) are various through-focal views captured to highlight both the multiple OAs (D, blue arrows) and the multiple CVP sets (red arrows, E and F).

Though it is attractive to postulate that over-expression of a JanA-gene product affects mechanisms that regulate Anterior/Posterior polarity in the cell, the authors suspect this result is more likely an attempt on the part of the cell, to re-integrate the multiple (failed) division products such as those seen in Fig. 8G. Continued JanA/CDC5:GFP over-expression results in some rather spectacular cyto-geometries, sometimes with ciliary rows folding back on themselves (highlighting the continued replication of basal bodies along each ciliary row).

The ‘terminal’ phenotype of *Tetrahymena* cells subjected to over-expression of the JanA/CDC5:GFP fusion protein.

Under continuous exposure to cadmium-driven *JanA/CDC5:GFP* over-expression (24 hours or longer), cells undergo multiple rounds of Mic division and basal body replication, while exhibiting cytokinesis failure. Typically these ‘monster’ phenotypes exhibit two MACs and two OAs, with a multitude of MICs and excess basal bodies (Fig. 11). Curiously, one of the final consequences of this over-expression phenotype, appears to be the complete loss of centrin from the somatic basal bodies. The antibody to centrin normally decorates the basal bodies that support the somatic and oral cilia, as well as a diffuse cytoplasmic cloud associated with the contractile vacuole system. Using the green CV assemblage as a positive control, as well as the persistent green centrin label over the oral membranelles, we confirmed that, though the *JanA/CDC5:GFP* marker remains in linear punctae associated with ciliary rows, these punctae are now negative for centrin labeling.

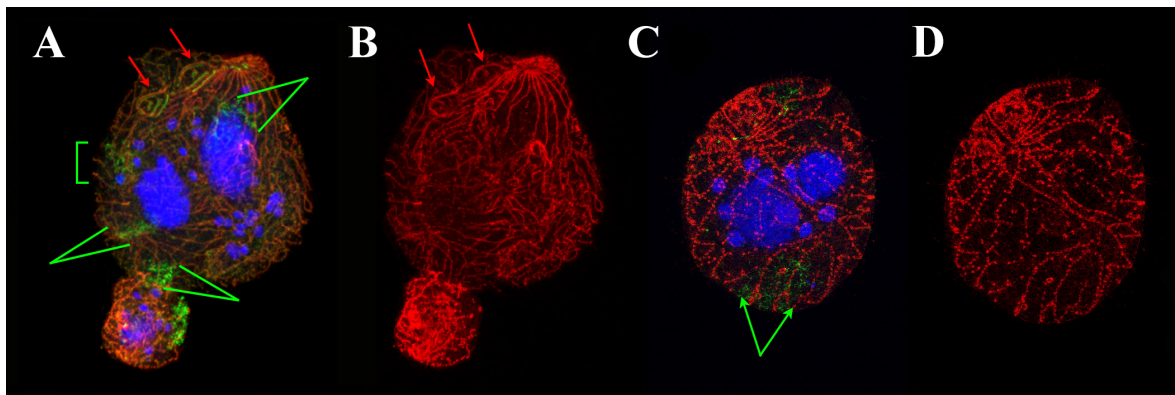


Figure 11. *Tetrahymena* cells following 8-24 hours of induced over-expression of the *JanA/CDC5:GFP* fusion protein. Red indicates the *JanA/CDC5:GFP* fusion protein highlighted with an antibody to GFP. Green = antibody to centrin decorating basal bodies and the contractile vacuole ‘complex’. Blue = DAPI staining of supernumerary MICs and MACs. A and B depict a ‘terminal phenotype’ in which the MAC has divided once, two OA are conspicuous (red arrows) and there are numerous MICs.

Pharmacological effects of the drug volasertib that blocks PLK activity.

Having identified the *Tetrahymena* JanA-1/CDC5 gene product as a Polo-like, Ser-Thr kinase homologous to the cell-cycle master control gene found in vertebrates, we were curious to learn if the JanA-1 gene product was sensitive to drugs developed as potential anti-cancer treatments that antagonize PLK activity (Steegmaier, et al., 2007; Gjertsen, & Schöffski 2015). We tested two of these: volasertib and BI2536. Cells were cultured overnight in a range of drug concentrations, and cortical features were examined following brief expression of the MTT-driven *JanA/CDC5*:GFP fusion gene. CVP numbers provide a convenient measure of the strength of the drug effect, and Oral Assembly allows assessment of the more extreme phenocopies. Figure 12 shows the dose-response for varying concentrations of volasertib on cortical patterning as assessed by CVP count.

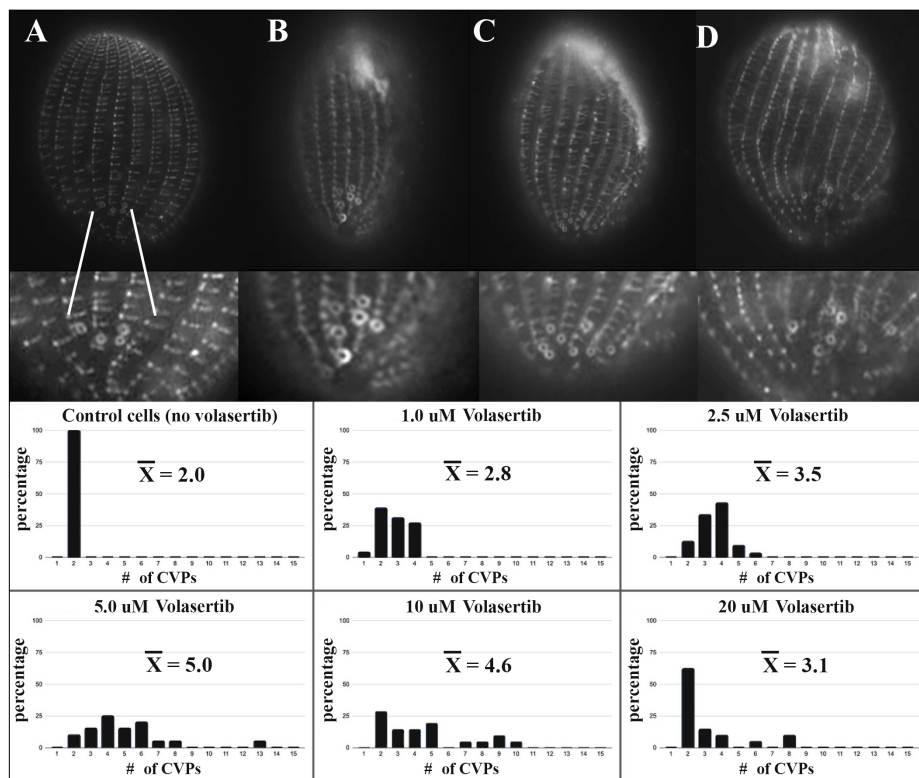


Figure 12. Wildtype cells (CU428) treated overnight to a range of volasertib concentrations, and imaged following brief expression of the MTT:JanA/CDC5:GFP fusion gene with 2.0 ug/mL CdCl₂. Four examples from the 5.0 uM treatment are shown expressing four, six, eight and ten CVPs (Figs. A-D). 5.0 uM volasertib gave the most consistently high number of CVPs with one example expressing 13 CVPs instead of the typical two.

The CVP phenotype expressed in volasertib-treated cells was not what we expected. When the JanA/CDC5 gene product is progressively removed by mutant gene suppression from a wildtype cell, we see a modest broadening of the CVP domain from 2 CVPs to 3 or occasionally 4. This

broadened field of CVPs often becomes divided by a gap of one unoccupied ciliary row (See Fig. 2). Volasertib created a profound expansion of the CVP-domain, more than doubling its average width at the optimal concentration (5.0 uM), and producing examples with as many as 13 CVPs, a phenotype never observed in *janA* mutants. Curiously, the CVP-broadening phenocopy became less severe at higher concentrations. We suspect that this is due to progressively more severe suppression of cell division at higher concentrations, preventing assembly of new CVP fields under the influence of the drug. In such cases one sees, increasingly, just the persistent ‘parental’ CVP domain of non-dividing cells.

Only rarely did CU428 cells exhibiting signs of a second OP developing 180 degrees around the dorsal surface in response to volasertib. It is noteworthy, that the volasertib-treatment didn’t simply ‘broaden’ the cell’s CVP domain (causing CVPs to assemble alongside an increased number of ciliary rows), the CVP domain was expanded along the anterior-posterior axis of a ciliary row as well, with 2-3 CVPs seen alongside a single kinety (See Fig. 12 B). Hence, it is more accurate to state that volasertib expands the CVP domain both laterally and longitudinally. These results suggest that the *janA* mutation is partially, (though imperfectly) phenocopied by inhibiting all PLK activity in a wildtype cell. That said, broad-spectrum inhibition unambiguously implicates PLK activity in the control of the dimensions of the CVP domain, one component of the *janA* phenotype.

Pharmacological effects of BI2536, another PLK inhibitor on cortical pattern.

BI2536 produced an even stronger expansion of the CVP domain, with occasional cells exhibiting the janus global mirror-pattern duplication (Figs. 13, 14).

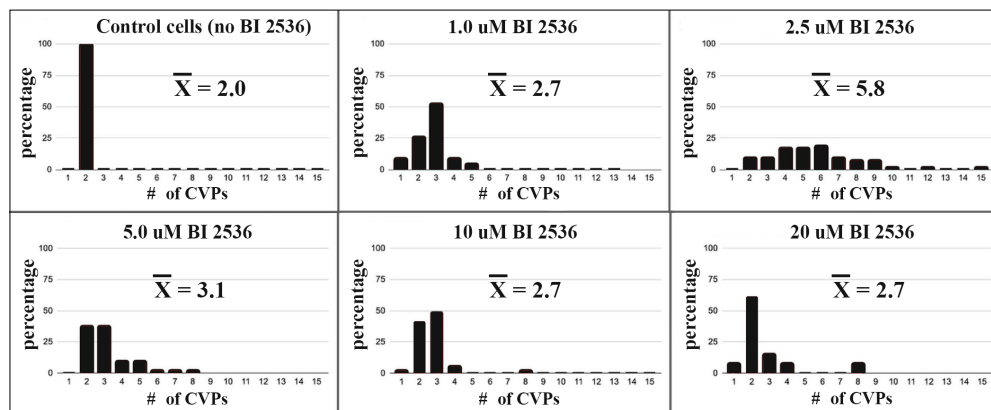


Figure 13. Wildtype cells (CU428) treated overnight to a range of BI2536 concentrations, and imaged following brief expression of the MTT:JanA/CDC5:GFP fusion gene with 2.0 ug/mL CdCl₂. 2.5 uM BI2536 gave the most consistently high number of CVPs with one example expressing 15 CVPs instead of the typical two.

The mirrored cortical pattern shown in Fig. 14 A-D, is remarkable in its similarity to the *janA* mutant phenotype suggesting that BI2536 is a more potent PLK inhibitor than volasertib in *Tetrahymena*, and is capable of producing a full janus phenocopy. Again the drug-induced phenocopy is unlike the *janA* phenotype in the sheer over-abundance of CVPs (Fig. 14E) and in the unexpected multiplication of the cell's cytoprocts. Wildtype cells have a single cytoprot slit (Fig. 14 E), whereas BI2536-treated cells could display 4 or even 5 (Fig. 14F).

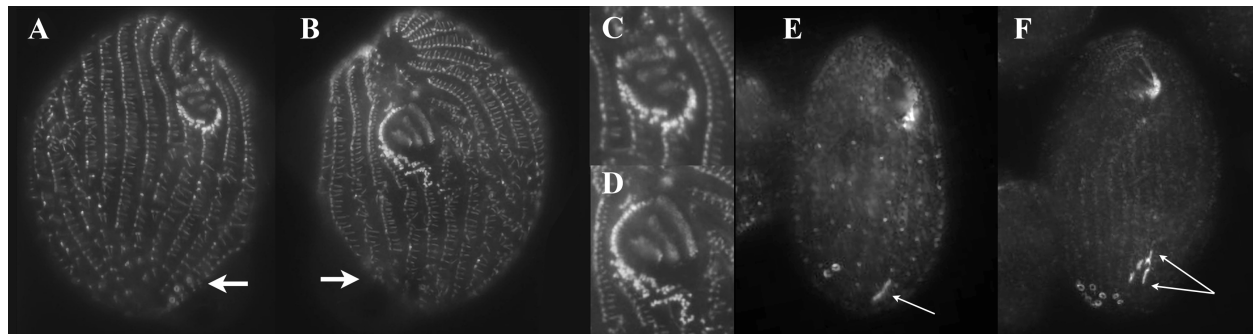


Figure 14. *eja* cells expressing the JanA/CDC5:GFP fusion-protein and grown under the influence of 2.5uM BI2536. A) The dorsal view, showing an OA with partial reversal of local asymmetry (expanded view in C). A CVP domain is visible lower right (arrow). Notably, this CVP domain is on the cell's left of the secondary OA and to the cell's right of the primary OA. B) The ventral view showing a more normal primary OA. Both OAs exhibit some evidence of UM disassembly typical of oral replacement. D) An expanded view of the primary OA seen in Fig B. Note, we used the intrinsic asymmetry of the transverse microtubules for orientation, printing images as they would appear from each surface, rather than the reverse image one would observe of the back of the cell as one down-focusses through the specimen. (Transverse microtubules extend to the cell's-left, viewer's right of each ciliary row). E) A wildtype cell labeled with antibody to fenestrin (a protein that decorates CVPs and the Cytoprot: Cyp). Arrow indicates the single Cyp. F) *eja* cells expressing the JanA/CDC5:GFP fusion-protein and grown under the influence of 2.5uM BI2536. This cell exhibits 7 CVPs and at least four Cyps (arrows).

PLK inhibition by BI2536 creates a more extreme phenocopy in cells homozygous for *eja*.

As we learned from studying the *janA1* mutants, the *janA* phenotype is enhanced when expressed in cells homozygous for a 2nd-site phenotype enhancer, *eja*. We compared the effect of 2.5uM BI2536 on CU428 cells (without the *eja* mutation) with that on IA264 cells (cells homozygous for *eja*). Some results appear in Fig. 15. BI2536 produced almost 1.5 times more CVPs in cells that were homozygous for the *enhancer of janA* mutation.

We also observed abnormal features in the OAs of BI2536-treated *eja* cells (Fig. 16). The OAs frequently displayed a disorganized field of basal bodies where the tight, double row of the undulating membrane (UM) should be, and frequently adopted a mirrored configuration of primary membranelles 1-3 (Figs. 16 C-E). This same mirrored configuration was seen in BI2536-treated wildtype cells, though to a lesser extent. The mirrored-membranelle form, though highly consistent in treated *eja* cells, is difficult to interpret. In such cells, the UM

appears to have dissociated into an anarchic field of basal bodies (Fig 16 B) reminiscent of the oral replacement primordium (ORP) described earlier following JanA/CDC5-over-expression (Fig. 8A).

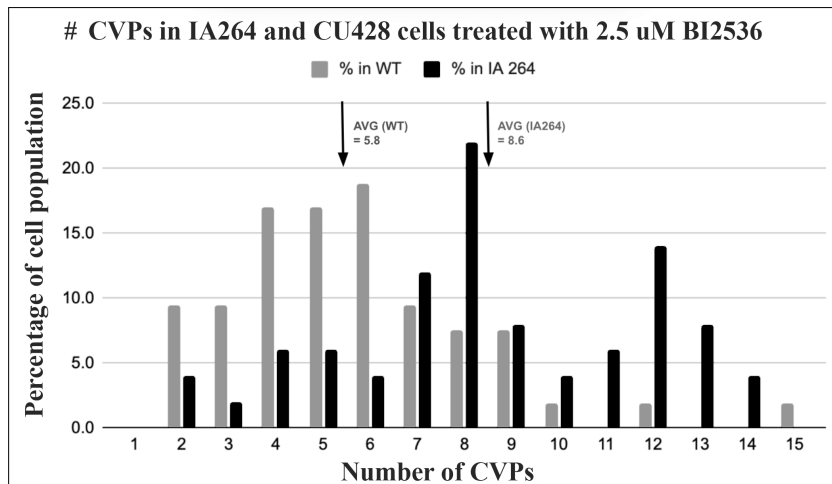


Figure 15. CVPs were counted in two different cell lines treated overnight with 2.5uM BI2536. CU428 was used as a wildtype control and the IA264 cell line is homozygous for the *eja* mutation. BI2536 had a significantly greater effect on CVP domain-broadening in the *eja* mutant (T-test result: $p < 1.3 \times 10^{-6}$).

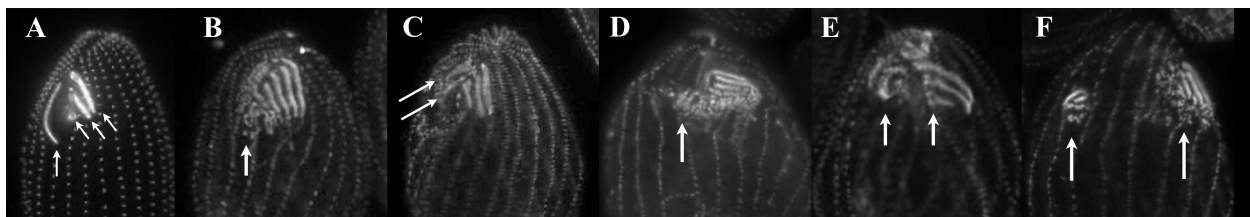


Figure 16. The effect of BI2536 on the OA of IA264 cells (homozygous for *eja*). A) A wildtype OA labeled with Poc1:GFP (photo courtesy of Chad Pearson). Vertical arrow is pointing to the UM (undulating membrane). Diagonal arrows indicate membranelles 1,2 and 3. B) IA264 cell exposed to BI2536 showing a dispersed field of basal bodies where the UM should be. C) Basal bodies in the region normally occupied by the UM appear to be organizing into rows angling upward from lower left to upper right (arrows). D) Appearance of what appears to be a 2nd OA (arrow) to the viewer's left of the primary OA, with membranelles angling from lower left to upper right. E) Even more discrete secondary OA (left arrow). Note, primary OA (right arrow) is still lacking a UM. F) Two discrete OAs separated by three ciliary rows. The primary, right-most OA still lacks a well-organized UM.

During oral replacement, the UM dissociates, creating a field of basal bodies. These basal bodies join others proliferating from the anterior-most region of the first post-oral ciliary row. In wildtype cells, this proliferating ORP field of basal bodies (similar to the OP that forms at midbody during pre-division morphogenesis), organizes into a new OA located posterior to the original OA. The latter undergoes disassembly and presumably, endocytic resorption.

In BI2536-treated *eja* cells, this loosely organized field of basal bodies frequently assembles into what appears to be a 2nd OA situated lateral to the primary, newly assembled OA, (Figs. 16

C,D,E) and assembled with superficial mirror-symmetry to the first. Membranelles of the second OA angle from lower left to upper right, rather than normally from lower right, to upper left ([viewer's perspective](#)). This UM disruption coupled with a mirrored-symmetry of the membranelles was observed for both dorsal and ventral OAs in the full-janus phenocopies as well (Figs. 14 A-D).

The identity of the mirrored membranelles in the OA to the viewer's left within the 'chevron' pattern, was uncertain. They were almost always underdeveloped, and it could not be discerned with confidence whether these represented a set of supernumerary UMs as seen in the misaligned undulating membrane mutant, *mum*, (Lansing et al., 1985), or the primary membranelles, M1-M3 (See Fig. 17). In order to discern the identity of membranelles from both left and right halves of the mirror-symmetric OAs, we raised cells expressing a novel GFP marker: an *MPH*:GFP fusion gene expressed from the *MPH* endogenous promoter. The *MPH* gene was first inferred by Frankel's characterization of the *mpH* mutant that produces two rather than three primary membranelles within the OA, (Frankel, 2008). The *MPH* gene was only recently identified ([Gaertig et al. in preparation](#)). The *MPH*:GFP fusion product specifically decorates the primary oral membranelles (M1, M2, M3) and distinctly fails to decorate basal bodies of the UM ([Gaertig, unpublished results](#)).

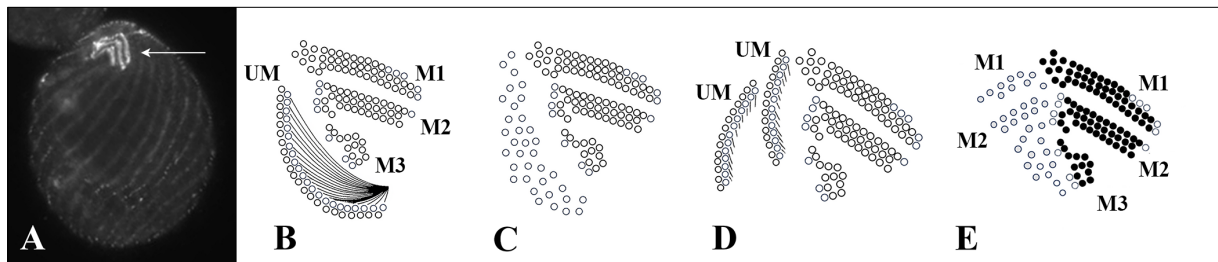


Figure 17. A) An IA264 (*eja*) cell labeled with anti-centrin, under the influence of 2.5 uM BI2536. Note the 'chevron' shaped OA (arrow). B) A schematic diagram detailing the wildtype OA showing M1, M2, M3 and the UM. C) A diagram of an *eja* cell under the influence of 2.5 uM BI2536 showing dissociated basal bodies in place of UM. D) One possible interpretation of the 'chevron' configuration would be that it represents a *mum* mutant phenocopy (Lansing, et al., 1985). The membranelles on the left half of the chevron would then represent supernumerary UMs. E) An alternative interpretation of the 'chevron' configuration is that there is a mirrored-duplication of the primary membranelles, M1-M3.

When MPH:GFP is expressed in wildtype cells and these cells are incubated overnight with 2.5uM BI2536, we made several unambiguous observations (Fig. 18). First, many cells appeared to be undergoing oral replacement regardless of whether they were raised in nutrient or non-nutrient medium (Fig. 18B). Second, basal bodies that comprise the ORP were decorated with

MPH just as the M1-M3 basal bodies of the mature, wildtype OA are. Third, the UMs of OAs from drug-treated cells appear to be dissociated or non-existent (Figs. 16 and 17C), and fourth, in cells exhibiting the ‘mirrored-membranelle’ pattern, the basal bodies are labeled with MPH:GFP on both sides of the line of symmetry identifying them as primary membranelles, (M1-M3) and not as UMs (Figs. 17E, and 18 E and F).

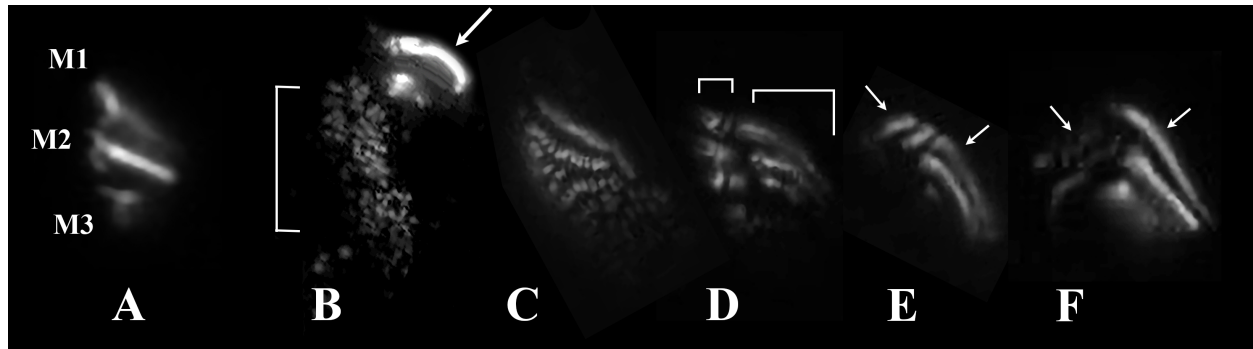


Figure 18. A) The OA of a CU428 (wildtype) cell expressing the MPH:GFP fusion protein that decorates basal bodies in the three primary membranelles, M1-M3. Note, no label appears over the UM. B) The OA from similar cells exposed overnight to 2.5 uM BI2536. A field of proliferating basal bodies is labeled (bracket) just posterior to degenerating membranelles, M1 and M2 (arrow). C) The presumed ORP organizing into pro-membranelle rows of bb doublets. D) Two discrete fields of membranelles organized side-by-side (brackets). E, F) Examples of a mature OA in which two sets of membranelles have assembled orthogonally to one another in superficial mirror-symmetry (arrows).

Discussion

We present evidence positively identifying the gene responsible for the *Tetrahymena* mirror-image pattern mutant, *janA*. We identified the gene by next-generation sequencing, and confirmed its identity both by creating a deletion of the wildtype gene and reproducing the *janA* phenotype, and by sequencing a 2nd *janA1-2* allele, and demonstrating that both alleles exhibit base pair changes in the presumed *JanA* locus at the same chromosomal locus identified by classic complementation tests involving nullisomic cell lines. The gene sequence is homologous to Human *PLK3* and the yeast *CDC5*, genes that encode a polo-like kinase.

The wild-type gene was then fused to a GFP sequence and expressed downstream from either the endogenous *JanA* promoter, or the cadmium-inducible *MTT1* promoter. When expressed from the endogenous promoter, or from the inducible promoter absent cadmium, (allowing only modest ‘leak’ expression from the uninduced *MTT1* promoter), localization was consistent. The JanA:GFP fusion protein is targeted to basal bodies restricted to the dorsal hemi-cell, a region usually devoid of the ventral suite of cortical organelles including the OA, CVPs and cytoproct.

When expressed for 2-4 hours, the MTT-driven JanA:GFP fusion protein spreads to decorate all the basal bodies (dorsal and ventral) as well as the OA, OP and CVPs. Brief induction (less than 2 hrs) has little impact on the cell's cortical pattern raising the possibility of using this construct in live cells as a 'cortical pattern reporter' for studying ciliate pattern processes.

Continued expression from the MTT-promoter triggers a progressive suite of cortical abnormalities that we interpret as an over-expression phenotype. It cannot be ruled out that these abnormalities are due to the mutant nature of the GFP-tagged protein acting as a 'poison product', and not simply JanA-over-expression. The progressive 'over-expression' phenotype is initiated by triggering oral replacement, a developmental program normally seen only in cells undergoing nutrient deprivation (Frankel, 1969, 1970; Nelsen, 1978). Following subsequent rounds of cell division under induced fusion-gene overexpression, there is a diminution of the CVP domain from the normal two CVPs to one or possibly even elimination of CVPs altogether, doubtless a lethal phenotype. Oral assembly appears to be compromised as well, and cells begin to exhibit cytokinesis failure and failure of MAC division. Curiously, MIC divisions seem to proceed normally as does basal body replication along the ciliary rows. Following a failed attempt at cytokinesis, the resultant 'monsters' frequently attempt some form of cortical integration. Ultimately, basal bodies lose the ability to bind anti-centrin antibodies.

The fact that JanA is a polo-like kinase, raised the possibility that drugs targeting PLK in metazoans might be effective at suppressing this Ser/Thr kinase activity in *Tetrahymena*. We tested the effect of volasertib and BI2536 on cortical patterning in wildtype cells expressing the MTT-driven JanA:GFP cortical reporter. Both drugs induced a dramatic expansion of the CVP and for BI2536 (at least) Cyp domains in wildtype cells. BI2536 showed a more extreme effect on CVP domain, and cells were occasionally found with a global, mirror-duplication of the ventral pattern of cortical organelles (the janus phenocopy). When BI2536 was applied to IA264 (a cell line homozygous for the 2nd-site enhancer of *janA: eja*), the influence over CVP production was significantly more extreme than when wildtype cells were treated. There appeared to be an enigmatic effect on the OA as well. The UM appeared dissociated, often replaced with or reorganized into a mirror-duplication of the primary OA with membranelles adopting the opposite slant within the organelle. The OA from these cells appeared most commonly as a 'chevron'. Occasionally, there was a gap separating a primary OA from a less developed secondary OA, again, frequently exhibiting a mirrored orientation of the

membranelles. Fully mirrored *janus* phenocopies were also observed, and their oral membranelles again had opposite, mirrored diagonal orientation to one another.

A model explaining the role of the JanA/CDC5/PLK protein in global, cortical patterning.

Three observations from this study offer insight into circumferential cortical patterning (C-patterning) within *Tetrahymena* cells. Loss of *JanA* function produces a global, mirror-image duplication of the cortical pattern of organelles normally assembled in the ventral hemi-cell. Endogenously driven *JanA*:GFP localizes strictly to the dorsal hemi-cell. Over-expression of the *JanA*:GFP fusion-protein diminishes (or eliminates) the CVP domain, and possibly disrupts OA development as well. It is tempting to invoke a role for the wildtype *JanA* gene product in suppressing a latent mirror-pattern of the ventral organelles within the dorsal cortex. This would suggest that the mirrored-pattern of cortical organelles represents a ground state or default option normally suppressed in the wildtype cell.

An easy model to envision, appears in Figure 19. In this model we invoke a symmetrical gradient of a cortical morphogen (turquoise) that diminishes with distance from some defined cortical meridian (the ‘source’).

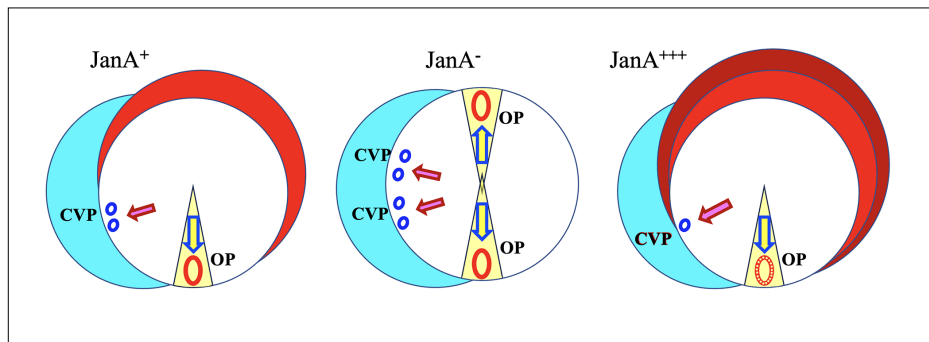


Figure 19. In this model of C-patterning in *Tetrahymena*, we hypothesize a completely theoretical cortical morphogen gradient (turquoise), spreading symmetrically from some key meridian. We place its source at approximately 9:00, viewing the polar projection as a clock. Striving for as simple a model as possible, we suggest that at high levels in this gradient, ciliary rows are licensed to assemble CVPs, while at lower concentrations (further from the source), a ciliary row is licensed to initiate basal body proliferation associated development of the OP. We then propose a proven distribution of the *JanA/CDC5* gene product (a polo-like kinase) distributed around the dorsal cortex (red). This kinase acts as a cortical repressor, inhibiting assembly of both CVPs and oral organelles. When the *JanA* gene product is eliminated (as in the *janA* mutants), the cortical repressor is removed, and ‘latent’ cues for organelle assembly are expressed symmetrically around the morphogen source. When one over-expresses the *JanA/CDC5* repressor, its cortical distribution expands (as observed), and the primary CVP domain, and oral assembly are disrupted.

A symmetric gradient with a high-point near 9:00 (viewing the polar projection as a clockface) could account for the mirrored/ symmetrical pattern observed in the *janA* loss of function

mutants. In the model displayed, the JanA/CDC5 gene product is depicted in red and acts as a cortical repressor, while an unidentified cortical morphogen (turquoise) spreads from its origin, licensing ciliary rows to form CVPs at its high point, and licensing (or permitting) basal body proliferation associated with oral assembly further from the source. Removing the JanA/CDC5 repressor allows symmetrical expression of the cortical morphogen, driving twin sets of CVPs and OPs at equivalent levels in the cortical morphogen gradient. Over-expression of the JanA/CDC5 fusion product causes lateral spread of the cortical repressor into the ventral hemi-cell, ultimately suppressing CVP formation and disrupting oral assembly.

Modeling the impact of broad-spectrum PLK inhibitors on cortical development.

Tetrahymena have five PLK homologs encoded in their genome, the JanA/CDC5 is only one of them. The PLK inhibitors we deployed (volasertib and BI2536) are notable for their general efficacy in suppressing PLK activity and likely interfere with multiple PLK pathways within our model organism. Consequently, drug effects on cortical morphogenesis cannot be specifically assigned to the JanA/Cdc5 gene product alone. Several features of the phenocopy produced using these drugs are notably different from the *janA/CDC5* loss-of-function mutant phenotype. First, PLK inhibition produces a wildly expanded field of CVPs. In the *janA1* mutations (both point mutations and the co-deletion strain), three or at most four CVPs assemble in side-by-side arrangement, or split into two fields separated by a ciliary row. Cells exposed to PLK inhibition express up to 15 CVPs, often assembling in vertical (anterior-posterior) clusters, two to three deep along a single ciliary row. These observations suggest that multiple drug-sensitive PLKs are involved in patterning the CVP domain, and wildtype PLK activity (writ large) appears to suppress CVP formation, as loss of PLK activity through either drug treatment or mutation results in expanded CVP production. We also observed multiplication of the cytoproct (Cyp) in cells under PLK inhibition.

There was also a curious derangement of the primary oral apparatus in cells treated with PLK inhibitors that is not seen in the *janA* mutants. The UM appears in a state of disassembly, with basal bodies only loosely associated. These loose basal bodies are often assembled into a second set of oral membranelles. This second set of membranelles are frequently organized in mirror-symmetric orientation to the first: a ‘local’ mirrored-symmetry affecting orientation within this complex cortical organelle.

In another mutant, *bcd1* (Cole et al., 1987, 2023), multiple OAs assemble side-by-side within the ciliate cortex. These side-by-side organelles do not show mirrored-symmetry in membranelle organization suggesting that this is not simply the result of a broadened oral domain recruiting neighboring ciliary rows to generate supernumerary oral primordia, but something specific to the local orientation within the developing organelle. One possibility is depicted in Fig. 20.

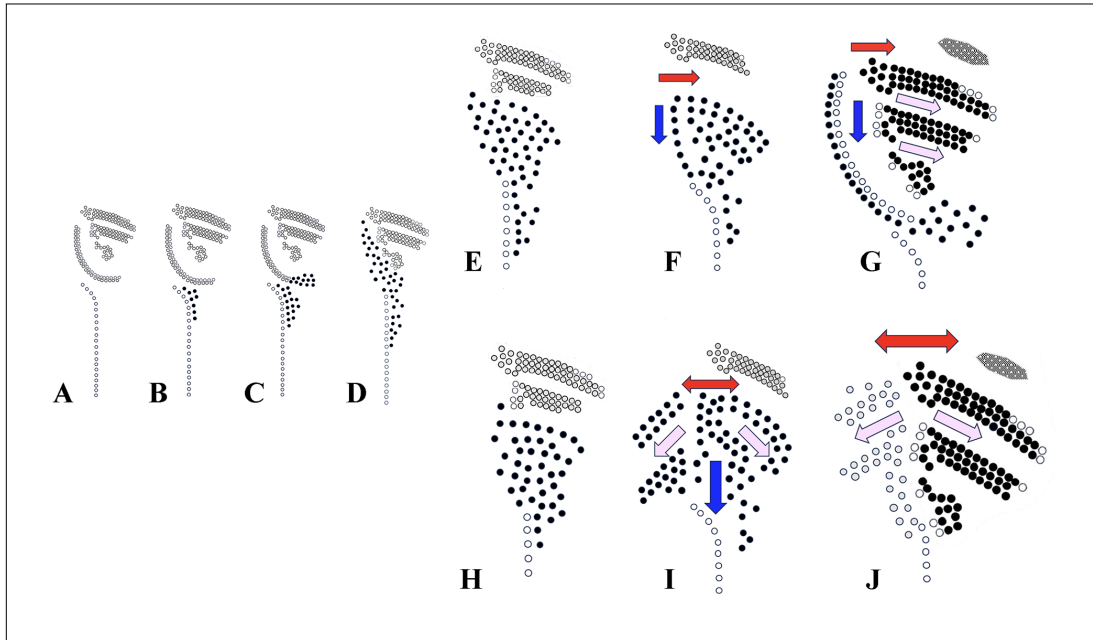


Figure 20. Oral replacement in a wildtype cell (A-G) and the curious ‘derangement’ of form in IA264 cells exposed to PLK inhibition using BI2536 (H-J). Parental basal bodies are depicted with open circles, while newly formed ORP basal bodies active in OA assembly are depicted as black filled circles (except in J, where left and right basal bodies are differentially filled or open for contrast). The oral replacement primordium (ORP) first appears as a field of basal body proliferation at the anterior end of the post-oral ciliary row (B). Shortly after, disassembly of the UM begins from the posterior end, and its basal bodies contribute to the proliferating field (C). The UM completely disassembles (D) and the ORP continues to replicate a field of basal bodies. One by one the primary membranelles (M1-M3) are either disassembled, or ultimately resorbed (E-G) (black arrow in figure G). As the parental membranelles are disassembled and resorbed, the ORP begins to form discrete, new membranelles (F,G). Membranelles assemble with distinctive asymmetry revealing organization along both the A/P axis and across the left/right field of symmetry. Our model suggests hypothetical ‘influences’ driving A/P organization within the developing membranelle field (Fig. F turquoise arrow) and left/right organization (red arrow) resulting in a combined ‘vectorial’ influence (G. pink arrows) manifesting as a diagonal orientation of the three primary membranelles and their anterior-right ‘sculpting’. We propose that inhibition of the cell’s PLK activity results in loss of polarity of the L/R ‘influence’, resulting in a symmetrical spread (double-red arrow, Fig. I). This results in a loss of UM assembly, and a mirrored set of primary membranelles (Figs. I, J).

In this model we suggest that PLK activity (in a wildtype/ control cell), is involved in driving left/right asymmetry within the developing ORP (the oral replacement primordium). In the absence of PLK activity, this chiral-patterning influence appears to spread symmetrically both to the left and right of the UM and the post-oral ciliary row whose basal bodies contribute to the newly formed primordium. The result appears to be loss of the UM, an organelle that typically

defines the left-most margin of the OA, and mirror-symmetric assembly of primary membranelles, M1-M3. In some sense, wildtype PLK activity appears to be serving as a firewall to an otherwise symmetric spread of OA-organizing activity, constraining its spread from the UM and post-oral meridian to the **cell's left**. When this firewall is abrogated by treatment with BI2536 (especially in cells homozygous for the *eja* mutation), this lateral patterning influence spreads symmetrically, creating a mirrored membranelle pattern or ‘chevron’ configuration. An open question is whether the mirrored-membranelle pattern emerges during mid-body development of the oral primordium, or is somehow expressed only during rounds of oral replacement that seem to be triggered by PLK inhibition.

Thoughts on Oral replacement and PLK activity.

The fact that PLK inhibitors trigger oral replacement (an alternative developmental program to cell division with its mid-body oral development), is interesting. Oral replacement involves breakdown and disassembly of an existing OA (presumably through endocytosis and autophagy) and replacement by a new one (Frankel, 1969; Nelsen, 1978). There may be two reasons for this. One of the five *Tetrahymena* PLKs may serve to repress this alternative, degradatory program unless triggered by amino acid starvation to permit it. In Humans, macro-autophagy has been linked to PLK activity in response to metabolic stress (Pang, et al., 2021, Zheng, et al., 2019). PLK1 has been demonstrated to exert an inhibitory influence over macro-autophagy, and PLK1 inhibition by RO3280 or BI2536 induces macro-autophagy partly via mTOR pathway dephosphorylation (Deeraksa et al., 2013; Tao, et al., 2017). It may be significant that the mTOR pathway is critical in monitoring amino acid and ‘energy’ levels in metazoans and other unicellular models, and in controlling cellular responses to nutritional down-regulation (including apoptosis/ autophagy). It seems reasonable to hypothesize, that one or more of the *Tetrahymena* PLK homologs may be playing a similar role in these cells, repressing a macro-autophagy pathway (oral replacement) unless the cell experiences amino-acid deprivation. Repression of this PLK could pharmacologically disinhibit the oral replacement pathway.

An alternative possibility, is that, as cells divide under conditions of PLK repression, oral development is impaired resulting in a non-functional OA. Nelsen demonstrated that during late stages of mid-body oral development, portions of the UM from the mature OA disassemble and then re-assemble in synchrony with the UM of the midbody OP (Nelsen, 1981). If PLK repression impairs proper OP assembly, it may simultaneously impair the integrity of the mature,

parental OA causing both daughter cells, the ‘proter’ inheriting the parental OA and the ‘opisthe’ inheriting a newly formed OA, to have defective mouths. This could lead to impaired feeding, which in turn triggers oral replacement.

Thoughts on a symmetric, mirrored oral apparatus and the evolution of cortical pattern.

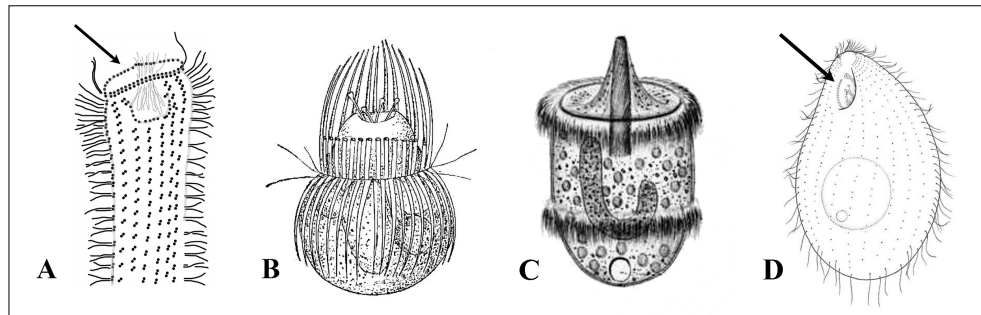


Figure 21. A) A Karyorelictid, an early divergent class of ciliate species showing a symmetrical OA that completely encircles the anterior aspect of the cell. (Modified from Foissner and Dragesco, 1996). B) *Mesodinium* another early divergent ciliate with a symmetrical, polar OA, (From Calkins, 1902). C) *Didinium*, a second ‘early divergent species from the class Litostomatea (From Stein, 1859). D) *Tetrahymena* exhibiting its asymmetric OA (from Lynn and Doerder, 2012).

On the face of it, it seems curious if not odd, that a loss-of-function mutation results not simply in a disarranged ventral pattern of organelles, but in a mirror-duplication of the ventral pattern on the dorsal surface. Furthermore, no fewer than three separate genetic loci (*JanA*, *JanB*, and *JanC*) appear necessary to maintain this derived ‘singlet’ morphology. It is hard to escape the impression, that the ‘default’ pattern for this ciliate: the developmental ground-state to borrow language developed from Ed Lewis’ studies on pattern mutants in *Drosophila* (Lewis, 1951; Lewis, 1978; Gehring et al., 2009), is a cell in which oral structures form on both the dorsal and ventral hemi-cells, and that the dorsal organelles were subsequently and robustly repressed. It may be significant, that the most early divergent ciliate species (some Karyorelictid species and most members of the class Litostomatea), exhibit symmetrical OAs, ones that circumscribe the entire anterior end of the cell. It is tempting to suppose that a symmetric OA represents the ancestral ciliate form, and that an asymmetric OA such as seen in *Tetrahymena*, and other Hymenostome Oligohymenophorea, is an evolutionarily derived form with members of the Janus gene family charged with suppressing dorsal stomatogenesis.

Methods

Strains

Cell lines used in this study:

SD00630: IA220 *janA-1/janA-1; ejal-1/ejal-1; chx1-1/chx1-1 (janA-1; ejal-1; chx1-1; janA, ejal, cy-r, II)*

SD00631: IA221 *janA-1/janA-1; ejal-1/ejal-1; chx1-1/chx1-1 (janA-1; ejal-1; chx1-1; janA, ejal, cy-r, III)*

SD00643: IA385 *janA-2/janA-2; ejal-1/ejal-1 (janA-2; ejal-1; janA, ejal, II)*

SD00644: IA387 *janA-2/janA-2; ejal-1/ejal-1 (janA-2; ejal-1; janA, ejal, V)*

SD00178: CU428 *mpr1-1/mpr1-1 (MPR1; mp-s, VII)*

SD00632: IA264 *gal1-1/gal1-1; ejal-1/ejal-1* (*GAL1; ejal-1; gal-s, ejal, II*)

SD00015: A-star III

SD00022: B-star VI

All strains provided by the *Tetrahymena* Stock Center now housed at Washington University, St. Louis. <https://sites.wustl.edu/tetrahymena/> (formerly: <https://tetrahymena.vet.cornell.edu/>).

Cell Culture Conditions

Cells were grown at 30°C in ‘NEFF’ (SPP?) medium (0.25% proteose peptone, 0.25% dextrose, 0.5% yeast extract, 0.009% ferric EDTA). Matings were conducted using Dryl’s starvation medium medium (Dryl, 1959) (2 mM NaPO₄ buffer, 2 mM sodium citrate, 1.5 mM CaCl₂ pH 7.1).

Identification of the *JanA-1* mutation Jacek

A mutant *T. thermophila* strain homozygous for *janA-1* and *CHX-1* (IA220- RRID TSC_SD00630) was outcrossed to CU428-RRID TSC_SD00178 (a 6-methyl purine-resistant heterokaryon), and the double drug-resistant (6-methylpurine [6mp] and cycloheximide [cy]) F1 progeny clones were selected. Several F1s were propagated vegetatively, and cy-sensitive ‘macronuclear assortant’ clones were identified by replica plating. To obtain clones homozygous for either *janA-1* or WT JanA1, we used the method of ‘uniparental cytogamy’ (Cole, et al., 1992). A single cy-sensitive F1 was grown and crossed to B*VI and the mating culture was exposed to a hyper-osmotic shock a 5.75 hrs into mating at 30°C. The shocked pairs were diluted and distributed to microtiter plates with Neff media to recover. 24 hrs later, cycloheximide was delivered (12.5 µg/ml), and CyR survivors identified after four days in drug. 367 drug resistant syncclones were identified. These were screened by eye for janus-mutant appearance (slow-growing and abnormal shape), and screened again with high-resolution, DIC microscopy for the appearance of secondary OAs. 32 confirmed *janA* mutants were identified and 41 confirmed wildtypes.

WT and mutant F2 progeny were pooled, and the pools were grown to a mid-log phase and starved for 2 d at room temperature in 60 mM Tris-HCl, pH 7.5. Total genomic DNA was extracted using the urea method (Dave et al., 2009). The pool DNAs were used to make genomic libraries using Illumina Truseq primer adapters and sequenced on an Illumina HiSeq X instrument, which generated paired-end reads of 150-base-pair length at 90× genome coverage. The MiModD suite of tools version 0.1.8 (<https://sourceforge.net/projects/mimodd/>) was used for ACCA-based variant mapping and identification (Jiang et al., 2017) as follows. The sequencing

reads were aligned to the micronuclear reference genome (GenBank assembly accession **GCA_000261185.1**; Hamilton *et al.*, 2016), and the aligned reads from both pools were used for joint multi-sample variant calling. The variant call data set was filtered for sites with high coverage for each of the two pools. Linkage scores contrasting the allelic composition of the mutant with that of the WT pool were computed for each variant and the results plotted against micronuclear genome coordinates. For variant identification, the same sequencing reads were aligned to the macronuclear reference genome (GenBank assembly accession **GCA_000189635** (Eisen *et al.*, 2006) and the aligned reads subjected to variant calling as above.

To create a null macronuclear allele for *TTHERM_00191790*, we used the ‘codeletion’ method based on expression of scan RNAs that target the genome in the developing macronucleus for deletion (Hayashi and Mochizuki, 2015). An ### -base-pair fragment of *TTHERM_00191790* (located between positions ### and ### base pairs of the predicted coding region) was cloned into the *NotI* site of the pMcode1 rDNA vector using Gibson Assembly. The resulting pMcode1-JanA-1 plasmid was introduced into mating B2086 and CU428 *Tetrahymena* cells (at ~8 h after mixing of the two strains at 30°C) using biolistic bombardment (Cassidy-Hanley *et al.*, 1997). Transformants were selected in supplemented proteose peptone medium (SPP; 2% proteose peptone, 0.1% yeast extract, 0.2% glucose, 33 µM FeCl₃) with 100 mg/ml paromomycin. ### independent “codel” clones were isolated and all confirmed to contain deletions in the targeted region using primers with sequences located outside of the *NotI* insertion site, within the sequence of rDNA. We analyzed the co-del Δ strain.

Identification of janA-2 mutant allele

Jacek

GFP tagging

janA and MPH.

Jacek

Immunofluorescence imaging.

Cells were fixed and stained with antibodies as described by (Jiang *et al.*, 2020). Samples were air-dried at 30°C, the cover glass was washed three times with PBS and incubated with primary antibodies diluted in PBS supplemented with 3% BSA fraction V and 0.01% Tween-20. The primary antibodies used were: polyclonal anti-GFP (Rockland; 1:800 dilution), monoclonal

anti-centrin 20H5 (EMD Millipore; 1:400; Salisbury et al., 1988), and monoclonal anti-fenestrin (3A7) (Nelsen et al., 1994). The latter is now available from the DSHB located at the University of Iowa. The secondary antibodies were conjugated to either TRITC or FITC (Rockland; 1:300). The nuclei were co-stained with DAPI (Sigma-Aldrich). The labeled cells were embedded in VectaShield anti-quenching mounting medium for fluorescence (VectorLabs).

Microscopy

Cells were imaged using an Olympus BX50 fluorescence microscope and a C-Mos digital camera. **SIM (Jacek text)**.

Drug treatment

Volasertib, (BI6727) was obtained from Sigma-Aldrich and dissolved in DMSO creating a 1mM concentrate. 10mM BI2536 in DMSO was obtained from Thermo Scientific. We diluted it to a 1mM solution to create a stock solution. These stock solutions were then diluted into cell cultures to create the range of final concentrations.

Acknowledgments: Research in the Cole laboratory was supported by NSF #1947608. Research in Gaertig lab was supported by the NIH grant 5R01GM135444. We appreciate the assistance of Liana R.X. Cole, in helping discern the Janus form from the microscopically similar, parabiotic-doublet form, and Kathleen R. Stuart for assistance in screening for monoclonal antibodies of the fenestrin antibody. This article is dedicated to the years of fine investigative work conducted in the laboratory of Professor Joseph Frankel, University of Iowa.

Literature cited

- Bruns, P. J., Brussard, T. B., & Kavka, A. B. (1976). Isolation of homozygous mutants after induced self-fertilization in *Tetrahymena*. *Proceedings of the National Academy of Sciences*, 73(9), 3243-3247.
- Bruns, P. J., Brussard, T. B., & Merriam, E. V. (1983). Nullisomic *Tetrahymena*: A set of nullisomics define the germinal chromosomes. *Genetics*, 104, 257-270.
- Bruns, P. J., & Sanford, Y. M. (1978). Mass isolation and fertility testing of temperature-sensitive mutants in *Tetrahymena*. *Proceedings of the National Academy of Sciences*, 75(7), 3355-3358.
- Calkins, G. (1902). Marine Protozoa from Woods Hole, Bulletin of the United States Fish Commission. Vol. 21, 1901.
- Cassidy-Hanley, D., Yao, M. C., & Bruns, P. J. (1994). A method for mapping germ line sequences in *Tetrahymena thermophila* using the polymerase chain reaction. *Genetics*, 137(1), 95-106.
- Cassidy-Hanley, D., Bowen, J., Lee, J. H., Cole, E., VerPlank, L. A., Gaertig, J., Gorovsky, M. A., & Bruns, P. J. (1997). Germline and somatic transformation of mating *Tetrahymena thermophila* by particle bombardment. *Genetics*, 146(1), 135-147.
<http://www.ncbi.nlm.nih.gov/pmc/articles/PMC1207932/pdf/ge1461135.pdf>
- Cole, E. S., & Frankel, J. (1991). Conjugal blocks in *Tetrahymena* pattern mutants and their cytoplasmic rescue: II. janus A. *Developmental biology*, 148(2), 420-428.
- Cole, E. S., & Bruns, P. J. (1992). Uniparental cytogamy: a novel method for bringing micronuclear mutations of *Tetrahymena* into homozygous macronuclear expression with precocious sexual maturity. *Genetics*, 132(4), 1017-1031.
- Dave, D., Wloga, D., & Gaertig, J. (2009). Manipulating ciliary protein-encoding genes in *Tetrahymena thermophila* [Research Support, U.S. Gov't, Non-P.H.S.]. *Methods Cell Biol*, 93, 1-20. [https://doi.org/10.1016/S0091-679X\(08\)93001-6](https://doi.org/10.1016/S0091-679X(08)93001-6)
- Deeraksa, A., Pan, J., Sha, Y., Liu, X. D., Eissa, N. T., Lin, S. H., & Yu-Lee, L. Y. (2013). Plk1 is upregulated in androgen-insensitive prostate cancer cells and its inhibition leads to necroptosis. *Oncogene*, 32(24), 2973-2983.
- Dryl, S. (1959). Antigenic transformation in *Paramecium aurelia* after homologous antiserum treatment during autogamy and conjugation. *J. Protozool.*, 6, s96.
- Eisen, J. A., Coyne, R. S., Wu, M., Wu, D., Thiagarajan, M., Wortman, J. R., ... & Orias, E. (2006). Macronuclear genome sequence of the ciliate *Tetrahymena thermophila*, a model eukaryote. *PLoS biology*, 4(9), e286.

Foissner, W., & Dragesco, J. (1996). Updating the Trachelocercids (Ciliophora, Karyorelictea). I. A Detailed Description of the Infraciliature of *Trachelolophos gigas* NG, N. Sp. and T. filum (Dragesco & Dragesco Kernéis, 1986) N. Comb. *Journal of Eukaryotic Microbiology*, 43(1), 12-25.

Frankel, J. (1969). Participation of the undulating membrane in the formation of oral replacement primordia in *Tetrahymena pyriformis*. *J. Protozool.*, 16, 26-35.

Frankel, J. (1970). The synchronization of oral development without cell division in *Tetrahymena pyriformis* GL C. *Journal of Experimental Zoology*, 173(1), 79-99.

Frankel, J., & Jenkins, L. M. (1979). A mutant of *Tetrahymena thermophila* with a partial mirror-image duplication of cell surface pattern: II. Nature of genic control. *Development*, 49(1), 203-227.

Frankel, J., Jenkins, L. M., & Bakowska, J. (1984). Selective mirror-image reversal of ciliary patterns in *Tetrahymena thermophila* homozygous for a janus mutation. *Wilhelm Roux's archives of developmental biology*, 194, 107-120.

Frankel, J., & Nelsen, E. M. (1985). How the mirror image pattern specified by a janus mutation of *Tetrahymena thermophila* comes to expression. *Developmental genetics*, 6(3), 213-238.

Frankel, J., & Nelsen, E. M. (1986). Intracellular pattern reversal in *Tetrahymena thermophila*: II. Transient expression of a janus phenocopy in balanced doublets. *Developmental biology*, 114(1), 72-86.

Frankel, J., Nelsen, E. M., & Jenkins, L. M. (1987a). Intracellular pattern reversal in *Tetrahymena thermophila*: janus mutants and their geometrical phenocopies. In *Symp. Soc. Dev. Biol* (Vol. 45, pp. 219-244).

Frankel, J., & Nelsen, E. M. (1987b). Positional reorganization in compound janus cells of *Tetrahymena thermophila*. *Development*, 99(1), 51-68.

Frohnhofer, H. G., & Nüsslein-Volhard, C. (1987). Maternal genes required for the anterior localization of bicoid activity in the embryo of *Drosophila*. *Genes Dev*, 1, 880-890.

Gehring, W. J., Kloter, U., & Suga, H. (2009). Evolution of the Hox gene complex from an evolutionary ground state. *Current topics in developmental biology*, 88, 35-61.

Gjertsen, B. T., & Schöffski, P. (2015). Discovery and development of the Polo-like kinase inhibitor volasertib in cancer therapy. *Leukemia*, 29(1), 11-19.

Hamilton, E. P., Kapusta, A., Huvos, P. E., Bidwell, S. L., Zafar, N., Tang, H., ... & Coyne, R. S. (2016). Structure of the germline genome of *Tetrahymena thermophila* and relationship to the massively rearranged somatic genome. *elife*, 5, e19090.

Hayashi, A., & Mochizuki, K. (2015). Targeted Gene Disruption by Ectopic Induction of DNA Elimination in *Tetrahymena*. *Genetics*, 201(1), 55-64.

Jerka-Dziadosz, M., & Frankel, J. (1979). A mutant of *Tetrahymena thermophila* with a partial mirror-image duplication of cell surface pattern: I. Analysis of the phenotype. *Development*, 49(1) 167-202.

Jiang, Y. Y., Maier, W., Baumeister, R., Minevich, G., Joachimiak, E., Ruan, Z., Kannan, N., Clarke, D., Frankel, J., & Gaertig, J. (2017). The Hippo Pathway Maintains the Equatorial Division Plane in the Ciliate *Tetrahymena*. *Genetics*, 206(2), 873-888.

<https://doi.org/10.1534/genetics.117.200766>

Lewis, E. B. (1951, January). Pseudoallelism and gene evolution. In *Cold Spring Harbor symposia on quantitative biology* (Vol. 16, pp. 159-174). Cold Spring Harbor Laboratory Press.

Lynn, D. H., & Doerder, F. P. (2012). The life and times of Tetrahymena. *Methods in cell biology*, 109, 9-27.

Miao W., Xiong J., Bowen J., Wang W., Liu Y.F., Braguinets O., Grigull J., Pearlman R.E., Orias E., Gorovsky M.A.: *Microarray Analyses of Gene Expression during the Tetrahymena thermophila Life Cycle*. *Plos One* 2009, 4(2).

Nelsen, E. M. (1978). Transformation in *Tetrahymena pyriformis*: Development of an inducible phenotype. *Dev. Biol.*, 66, 17-31.

Nelsen, E. M. (1981). The undulating membrane of Tetrahymena: formation and reconstruction. *Transactions of the American Microscopical Society*, 285-295.

Nelsen, E. M., & Frankel, J. (1986). Intracellular pattern reversal in *Tetrahymena thermophila*: I. Evidence for reverse intercalation in unbalanced doublets. *Developmental biology*, 114(1), 53-71.

Nelsen, E. M., & Frankel, J. (1989). Maintenance and regulation of cellular handedness in *Tetrahymena*. *Development*, 105(3), 457-471.

Nelsen, E. M., Williams, N. E., Yi, H., Knaak, J., & Frankel, J. (1994). "Fenestrin" and conjugation in *Tetrahymena thermophila*. *Journal of Eukaryotic Microbiology*, 41(5), 483-495.

Nüsslein-Volhard, C., & Wieschaus, E. (2003). Mutations affecting segment number and polarity in *Drosophila*. *A Cen. Nat.: Twenty-One Discover: Changed Sci. World*, 267.

Salisbury, J. L., Baron, A. T., & Sanders, M. A. (1988). The centrin-based cytoskeleton of *Chlamydomonas reinhardtii*: distribution in interphase and mitotic cells. *The Journal of cell biology*, 107(2), 635-641.

Shang, Y., Song, X., Bowen, J., Corstanje, R., Gao, Y., Gaertig, J., & Gorovsky, M. A. (2002). A robust inducible-repressible promoter greatly facilitates gene knockouts, conditional expression,

and overexpression of homologous and heterologous genes in *Tetrahymena thermophila*. *Proceedings of the National Academy of Sciences*, 99(6), 3734-3739.

Steegmaier, M., Hoffmann, M., Baum, A., Lénárt, P., Petronczki, M., Krššák, M., ... & Rettig, W. J. (2007). BI 2536, a potent and selective inhibitor of polo-like kinase 1, inhibits tumor growth in vivo. *Current biology*, 17(4), 316-322.

Stein, F. (1859). *Der organismus der infusionsthiere* (Vol. 1). W. Engelmann.

Tao, Y.F., Li, Z.H., Du, W.W., Xu, L.X., Ren, J.L., Li, X.L., Fang, F., Xie, Y., Li, M., Qian, G.H. and Li, Y.H., (2017). Inhibiting PLK1 induces autophagy of acute myeloid leukemia cells via mammalian target of rapamycin pathway dephosphorylation. *Oncology Reports*, 37(3), 1419-1429.

Williams, N.E., Frankel, J. (1973). Regulation of microtubules in *Tetrahymena* I. Electron microscopy of oral replacement. *J Cell Biol* 56:441-457.

Xiong, J., Lu, Y., Feng, J., Yuan, D., Tian, M., Chang, C. Fu, G. Wang, H. Zeng, and W. Miao. (2013). *Tetrahymena* functional genomics database (TetraFGD): an integrated resource for *Tetrahymena* functional genomics. *Database*, 2013, bat008.

Zheng, K., He, Z., Kitazato, K., & Wang, Y. (2019). Selective autophagy regulates cell cycle in cancer therapy. *Theranostics*, 9(1), 104.

>**ENSP00000361275**

Hsapieons SYN=PLK3, CNK, FNK, PRK, CNK, FNK, PRK, CNK, FNK, PRK
 NOTE=polo-like kinase 3 [Source:HGNC Symbol;Acc:2154]
 GENE=ENSG00000173846
 Length = 646

Score = 313 bits (801), Expect = 8e-85
 Identities = 201/607 (33%), Positives = 309/607 (50%), Gaps = 46/607 (7%)

Query: 41 FAKCYEVNLETXXXXXXXXXXQTLTKNRARQKLISEIKIHKSLNHQHVVAFEHVFEDH 100
 FA=CYE T+ ET + K R+K++EIT++H+ L H+H+V F H FED
 Sbjct: 73 FARCYEATDTETGSAYAVKVIPQSRVAKPHQREKILNEIELHRLDQHRHIVRFSHHFEDA 132

Query: 101 ENVYILLELCTNHTLNELIKRRKRLTELEVQCYVVQIVNALKYLHSHKVIHRLDKLGNLF 160
 +N+YI LELEC+ +L + K R L E EV+ Y+ QI++ LKYLY ++HRLDKLGN F
 Sbjct: 133 DNIYIFLELCSRKSLSAHIWKRHTLLEPEVRYYLQRQILSGLKYLHQRGILHRLDKLGNFF 192

Query: 161 LNEKMEIKLGFGLATKLEFDGKHTICGTPNYIAPEILDGKTGHSYQVDIWSLGVIY 220
 + E ME+K+GDFGLA +LE +K TICGTPNY+APE+L + GH + D+WSLG ++Y
 Sbjct: 193 ITENMELKVGDGLAARLEPPEQRKKTICGTPNYVAPEVL-LRQGHGPEADWSLGCVMY 251

Query: 221 TLLIGKPPFETPDVKTTYYKKIRNISYGFPE[N]PISDQARGLITRILNIDPQRRPTLDE[IM] 280
 TLL G PPPET D+K TY+ I+ + Y P+ +S AR L+ IL P+ RP++D+I+
 Sbjct: 252 TLLCGSPPFETADLKETYRCIKQVHYTL[PAS]—LSLPARQLLAAILRASPRDRPSIDQI 309

Query: 281 SSSFLNTGGTIPKVLPLATLACPPSASYTKOFLPQGNALKLNQAPMRLTDASQSTTNIK 340
 F G T P LP++ P + P A L ++ T ++
 Sbjct: 310 RHDFFTKGYT-PDRLPISSCVTVPDLT-----PPNPARSL-----FAKVTKSLF 352

Query: 341 G-KNASTSNLYSKQTTGAVPDASRPLGGTTSNNNQVSSQKDQRPQTQQFQKSDFKTSMS 399
 G K S ++ + +G V R G +D RP+ ++ +
 Sbjct: 353 GRKKKSKNHAQERDEVSGLVSGLMRTSVG-----HQDARPEAPAASGPAPVSLVE 402

Query: 400 TKNMGSGSQNPLFNQTNAPGLATAQSLXXXXXXXXXXXXXQKGFMQTGTQNFGKPVQP-- 457
 T S + L ++ G ++ FM QN QP
 Sbjct: 403 TAPEDSSPRGTL--ASSGDGFEEGLTVATVV/ESALCALRN CIAFMPPAEQNPAPLAQPEP 460

Query: 458 -VWVTQWVDYSAKYGLGYLLSNGCSGVFFFNDSTKVIDPTTNNIEYIERLGNERQDFVQQ 516
 VWV+-WVDYS K+G GY LS+ V FND T + L + Y N
 Sbjct: 461 LVWVSKWVWDYSNIKFGFGYQLSSRRVAVLFNDGTHMALSANRKTVHY----NPTSTKHFS 515

Query: 517 FTLKDYPPEMKKKVTLLSHFKSYLEEQMOKQNIQIEVPQFQGDLQPYVVKKWMKTKHAI 576
 F++ P ++ ++ +L +F SY+E+ + K V + + P + +W+KT A+
 Sbjct: 516 FSVGAVPRALQQLGILRYFASYMEQHLMKGGLDPSVEEV/EVPAPPPLL—QWVKTQDQAL 573

Query: 577 MFRLSNKIVQVSFQ-DKTEILLSS-ENKMTVYVDRKGTRTDYPLSTALE-SSNTEMSKRL 633
 + S+ VQV+F D T+++LS E +VT+V R + Y S + + ++ +RL
 Sbjct: 574 LMLFSGDTVQVNFYGDHTKLILSGWEPLLVTVARNRSACTYASHLRQLGCPDRLQRQL 633

Query: 634 KYTKDIL 640
 +Y +L
 Sbjct: 634 RYALRLL 640

Supplemental Figure #. PLK amino acid sequence from Human PLK3 compared with predicted protein from Tetrahymena CDC5/TTHERM_00191790. Red box indicates site of *janA-1 mutant allele*: W213→gained STOP codon. Blue box indicates site of *janA-2 mutant allele*: with a K185→frameshift.

TTHERM_00191790 (protein)

MDKANEGKDQLIIIEKISKVNGEMAVKKYLRGKLLGGFAKCYEVTNLETKKIAAKI
IPKQTLTKNRARQKLISEIKIHKSLNHQHVVAFEHVFDHENVYILLELCTNHTLNELIK
RRKRLTELEVQCYVVQIVNALKLHSHKVIRDLKLGFLNEKMEIKLGDFGLATKLEF
DGEKKHTICGTPNYIAPEILDGKTGHSYQVDIWSLGVIYTLILGKPPETPDVKTYKK
IRNISYGFPENVNPISDQARGLITRILNIDPQRRPTLDEIMSSFLNTGGTIPKVLPLATL
ACPPSASYTKQFLPQGNALKLNQAPMRLTDSASQSTTNIKGKNASTSNLYSKQTTGAVP
DASRPLGGTTSNWNQVSSQKDQRPQTQQFQKSDFKTSMSTKNMGSQSQNPLFNQTNAPGL
ATAQSLNTFTKTKNNFNSTQKGFMQTGTQNFGKPVQPVWVTQWVDYSAKYGLGYLLSNGC
SGVFFNDSTKVILDPTTNNIEYIERLGNERQDFVQQFTLKDYPPEMKKVTLLSHFKSYL
EEQMQKQNQNIQIEVPQFQGDLQPVYVKKWMKTKHAIMFRLSNKIVQVSQDKTEILLSS
NKMVTYVDRKGTRDYPLSTAESSNTEMSKRLKYTKDILTHMLNNNTNNNNGRGSMTN
VNPTQNGTEKENYN

Figure ##### The protein predicted from sequence analysis of the putative JanA gene locus. Turquoise = catalytic domain of a PLK: Serine/Threonine kinase. {Residues 28-285}. E-value: 2.15 e-168. Green = first polo-box. {Residues: 456-546}. E-value: 1.85 e-35. Yellow = second polo-box. {Residues: 564-643}. E-value: 3.56 e-30. Sites of *janA* mutations are indicated in magenta. The *janA-1* allele had gained a STOP codon at residue W213. The *janA-2* mutant allele exhibits a frameshift starting at K185.